Design strategies for pulse sequences in multidimensional optical spectroscopies

C. Scheurer[a] and S. Mukamel[b]
Department of Chemistry, University of Rochester, Rochester, New York 14627

(Received 20 February 2001; accepted 19 June 2001)

A unified description of resonant multiple-pulse experiments in coupled spin-$\frac{1}{2}$ systems in NMR spectroscopy and two-level systems in optical spectroscopy is presented. The connection between the NMR product operator formalism and the Liouville space pathways in optical spectroscopy is established. We show how the information obtained in various strong field two and three pulse NMR experiments can be extracted by combining heterodyne detected phase-controlled weak field signals generated at different directions. These results allow the design of sequences of weak optical pulses that accomplish the same goals as strong field multidimensional NMR spectroscopy. © *2001 American Institute of Physics.* [DOI: 10.1063/1.1391266]

I. INTRODUCTION

Multidimensional NMR spectroscopy has been a valuable and well established technique for over two decades. It allows us to probe structure and dynamics of molecules in great detail by manipulation of spin coherences in multiple pulse sequences, exploiting spin–spin interactions through chemical bonds or directly through space.[1,2] Optical spectroscopy has only recently reached a state where similar control over vibrational or electronic coherences is possible. This is due to the much shorter timescales involved that require ultrafast pulse techniques to perform coherent multidimensional optical spectroscopy. Pulse shaping and phase control of femtosecond pulses has been experimentally achieved over the last few years.[3] These ultrafast pulses have been used in various recent experiments to achieve multidimensional laser spectroscopy and the control and manipulation of vibrational and electronic coherences.[4–12] The theoretical description of optical multiple pulse spectroscopy was developed in parallel with the experimental techniques. The treatment of weak pulse experiments in terms of Liouville space pathways[13] has been successfully applied to propose new third- and fifth-order spectroscopies.[14] An alternative description of third-order spectroscopy is given by the Nonlinear Exciton Equations that allow to describe the nonlinear response of large aggregates of strongly coupled three-level systems.[15,16] These theoretical methods yield directly the nth-order response function which can be convoluted with n arbitrary envelopes of weak pulse fields to give the signal for any n-pulse experiment.[13] The calculation of the response function is typically rather involved due to its generality. An nth-order heterodyne experiment involves the control of n time intervals and thus constitutes an n-dimensional (nD) spectroscopy.[17] One is typically interested only in a comparatively low dimensional (2D, 3D) spectrum even if many more pulses are used to manipulate the coherences. This means that only a few of the possible time delays in a pulse sequence are varied and the decision which delays are varied should be based on the desired information and on a more detailed knowledge of the system that is studied.

The common way in which a 2D NMR pulse sequence is presented involves four distinct blocks: preparation, evolution, mixing, and detection.[18] The detection period yields one time domain and incrementing the evolution period yields the other time domain. The preparation sequence contains all pulses that are applied to the system before the first time domain which is incremented in consecutive experiments. The time delays between pulses in the preparation block are not changed and can be optimized to prepare the spin system in a specific initial nonequilibrium state. Similarly, the mixing sequence consists of all pulses between the evolution and the detection period and is also fixed. It serves to map the coherence pattern that evolved during the evolution period into a different pattern at the beginning of the detection period, thus revealing correlations in the system that is studied. In the simplest cases, preparation and mixing can consist of only a single pulse each. However, these simple techniques do not directly yield information about the system that would not be accessible by series of 1D experiments. The full power of 2D NMR becomes apparent if preparation and/or mixing consist of multiple pulses, creating and manipulating coherences in very specific ways, thus uncovering spin–spin interaction topologies.

Multidimensional spectroscopy is usually carried out on-resonance. This simplifies the theoretical description considerably since only few of the Liouville space pathways contributing to the nonlinear response functions dominate the response and should be retained. The theoretical tool developed to describe resonant multiple-pulse NMR spectroscopy is the product operator formalism (POF).[1,19] In the POF all pulses are assumed to be resonant and are described as mappings acting on an initial density matrix and yielding a transformed density matrix. The density matrix itself is expanded in a basis of spin-$\frac{1}{2}$ product states in which the action of pulses is especially simple to describe. The transformation

[a]Electronic mail: chris@feynman.chem.rochester.edu
[b]Electronic mail: mukamel@chem.rochester.edu

rules are given for all possible basis states. Similarly, the action of the free evolution Hamiltonian in the weak (isotropic) J-coupling limit, where the spin–spin coupling is smaller than the transition frequency differences, is also given in the form of transformation rules that contain the evolution time as a parameter. This formalism yields a very compact and efficient analytic description of pulsed experiments that has been the basis of most pulse sequence developments in liquid state NMR. The situation in optical spectroscopy is more complicated than in NMR for the lack of a Hamiltonian that is as general and universally valid as the spin-$\frac{1}{2}$ Hamiltonian of NMR. Yet the success of the POF makes it desirable to have a theoretical tool that is similar in its versatility for pulse sequence development in optical spectroscopy. The use of transformation rules for the density matrix evolution has several advantages over other approaches. It provides more insight into the generation of the spectroscopic signal and its dependence on the system Hamiltonian than purely numerical simulation schemes, since it yields an analytic expression for the signal that depends on the Hamiltonian parameters. It also allows a straightforward implementation of the algebraic transformation rules in computer algebra codes, making it easier to handle more complicated pulse sequences.

The closest analog to spin-$\frac{1}{2}$ NMR is optical spectroscopy of coupled two-level systems. These can be realized for electronic transitions (visible) or, approximately, for strongly anharmonic vibrational transitions (infrared). In this paper we develop the necessary operator mappings to describe resonant optical multiple pulse spectroscopy of weakly J-coupled two-level systems and study the similarities and differences between optical spectroscopy of two-level systems and NMR spectroscopy of spin-$\frac{1}{2}$ systems. Our aim is to show which coherence manipulations commonly used in NMR can be performed by weak optical fields. This includes phase cycling and coherence transfer pathway selection, which are effects achievable by macroscopic observation and therefore closely related to phase-matching and directional detection.[20] We will not consider strong optical pulses with finite flip angles[21] but rather develop a formalism for the limit of small perturbations by the pulse fields. Strong fields in laser spectroscopy affect the vibrational dynamics of the systems studied. This can be used to control the dynamics. In NMR, strong fields only affect the spin dynamics and due to the weak spin-vibrational coupling and the low pulse energies it is possible to observe unperturbed native molecular dynamics with strong fields in this case. To obtain similar information from laser spectroscopy we resort to weak field techniques. We will first compare the Hamiltonian of weakly J-coupled two level systems for optical spectroscopy with the commonly used liquid state NMR Hamiltonian. We then derive the necessary transformation rules for an operator treatment of optical spectroscopy in the weak field limit in analogy to the POF. Subsequently, we give a brief overview of some key ideas in 2D NMR and present important simple NMR pulse sequences: COSY (2D correlation spectroscopy), NOESY (2D Nuclear Overhauser Effect spectroscopy), 2D exchange spectroscopy, and double quantum spectroscopy. Based on the operator transformation rules we can describe optical three-pulse experiments in close analogy to NMR and identify optical weak field techniques that contain the same information as their NMR analogs. Appendix A summarizes some useful operator identities and properties to set the stage for the description of two-level systems. In Appendix B we survey in some detail the description of a single spin-$\frac{1}{2}$ in a magnetic field side by side with the analogous description of a two-level system in optical spectroscopy to make it easier to pinpoint the similarities and differences between both types of spectroscopies. Finally, Appendix C contains closed expressions for the optical response of an ensemble of weakly coupled two-level systems to a three-pulse sequence.

II. PARAMETRIZED HAMILTONIAN FOR COUPLED SPINS OR TWO-LEVEL SYSTEMS IN AN EXTERNAL FIELD

An optical two-level system labeled α is characterized by its transition frequency $\omega_\alpha = E_a - E_b$ (we use units in which $\hbar = 1$) between the two states under consideration ($|a\rangle$ and $|b\rangle$) and by the matrix elements of the dipole operator $\hat{P}$, i.e., the static dipole moments $\boldsymbol{\mu}^b = \langle b|\hat{P}|b\rangle$ and $\boldsymbol{\mu}^a = \langle a|\hat{P}|a\rangle$ and the transition dipole moment $\boldsymbol{\mu}^{ab} = \langle a|\hat{P}|b\rangle = \langle b|\hat{P}|a\rangle^\star$. Each of these matrix elements is given by a three-dimensional vector with x, y, and z components in a properly chosen coordinate system. The diagonal elements $\boldsymbol{\mu}^b$ and $\boldsymbol{\mu}^a$ are real due to the hermiticity of $\hat{P}$ while the transition dipole moment can, in general, be complex valued and we therefore define $\boldsymbol{\mu}^{ab} = \boldsymbol{\mu}^r + i\boldsymbol{\mu}^i$.

The most general form of the dipole operator for a two-level system is therefore given by

$$\boldsymbol{\mu} = \tfrac{1}{2}(\boldsymbol{\mu}^a + \boldsymbol{\mu}^b)\mathsf{I} + (\boldsymbol{\mu}^a - \boldsymbol{\mu}^b)\mathsf{I}_z + \boldsymbol{\mu}^r\mathsf{I}_x + \boldsymbol{\mu}^i\mathsf{I}_y, \tag{1}$$

where I_x, I_y, and I_z are spin-$\frac{1}{2}$ operators (Pauli matrices, see Appendix A) and we have used $\boldsymbol{\mu}$ to denote the dipole operator acting on the space of $\{|b\rangle, |a\rangle\}$ in analogy with NMR terminology (see Appendix B). In this equation all $\boldsymbol{\mu}$ with a superscript denote ordinary three-dimensional vectors and $\boldsymbol{\mu}$ is a vector of three 2×2-matrices. In terms of creation and annihilation operators Eq. (1) can be written as

$$\begin{aligned}\boldsymbol{\mu} = \tfrac{1}{2}((\boldsymbol{\mu}^a + \boldsymbol{\mu}^b)[\mathsf{B}^\dagger, \mathsf{B}]_+ + (\boldsymbol{\mu}^a - \boldsymbol{\mu}^b)[\mathsf{B}^\dagger, \mathsf{B}] \\ + \boldsymbol{\mu}^r(\mathsf{B}^\dagger + \mathsf{B}) - i\boldsymbol{\mu}^i(\mathsf{B}^\dagger - \mathsf{B})),\end{aligned} \tag{2}$$

where the creation and annihilation operators $\mathsf{B}^\dagger$ and B satisfy the Pauli commutation relationship given in Appendix A. Equation (2) can be recast in the more compact form

$$\boldsymbol{\mu} = \boldsymbol{\mu}^a\mathsf{B}^\dagger\mathsf{B} + \boldsymbol{\mu}^b\mathsf{B}\mathsf{B}^\dagger + \tfrac{1}{2}\,\boldsymbol{\mu}^{ab}\mathsf{B} + \tfrac{1}{2}\,\boldsymbol{\mu}^{ba}\mathsf{B}^\dagger. \tag{3}$$

The Hamiltonian symmetries and therefore the symmetry of the states $|b\rangle$ and $|a\rangle$ determine the properties of $\boldsymbol{\mu}$ and lead to considerable simplifications in the following cases:[22]

- For states $|b\rangle$ and $|a\rangle$ with well-defined and the same parity, only $\boldsymbol{\mu}^{ab} \neq 0$, while $\boldsymbol{\mu}^b = \boldsymbol{\mu}^a = 0$.
- If the Hamiltonian has rotational symmetry about one axis, say the z-axis, then M is a good quantum number and $\boldsymbol{\mu}^{ab}$ is a complex vector for transitions with $\Delta M = \pm 1$. Other-

wise the states $|b\rangle$ and $|a\rangle$ can always be represented by real wave functions and $\boldsymbol{\mu}^{ab}=\boldsymbol{\mu}^{r}$ is a real vector.

In NMR all spins align with respect to the external field and the magnetic moment depends isotropically on the spin. The magnetic moment operator of a spin-$\frac{1}{2}$ system contains therefore only one parameter (rather than four three-dimensional vectors) and is given by[23,24]

$$\boldsymbol{\mu}=\gamma\vec{\mathsf{I}}=\gamma(\mathbf{e}_x\mathsf{I}_x+\mathbf{e}_y\mathsf{I}_y+\mathbf{e}_z\mathsf{I}_z), \tag{4}$$

where γ is the gyromagnetic ratio and $\mathbf{e}_x$, $\mathbf{e}_y$, $\mathbf{e}_z$ are the unit vectors in the x, y, and z directions, respectively. Due to the high symmetry, the spin-$\frac{1}{2}$ system is more closely related to an atomic *sp*-transition in a strong electric field rather than to transitions in molecules. Equation (4) can also be recast in terms of the B, $\mathsf{B}^\dagger$ operators,

$$\boldsymbol{\mu}=\frac{\gamma}{2}((\mathbf{e}_x+i\mathbf{e}_y)\mathsf{B}+(\mathbf{e}_x-i\mathbf{e}_y)\mathsf{B}^\dagger+\mathbf{e}_z[\mathsf{B}^\dagger,\mathsf{B}]). \tag{5}$$

The general Hamiltonian of a single two-level system α in an electric field $\boldsymbol{\mathcal{E}}(t)$ is given by

$$\mathsf{H}_\alpha=\frac{\omega_\alpha}{2}[\mathsf{B}_\alpha^\dagger,\mathsf{B}_\alpha]-\boldsymbol{\mu}\cdot\boldsymbol{\mathcal{E}}(t), \tag{6}$$

where $\boldsymbol{\mathcal{E}}$ in optical spectroscopy usually is a linearly polarized field with frequency ω, amplitude $\boldsymbol{\mathcal{E}}_0(t)$ and phase $\phi=\mathbf{k}\cdot\mathbf{r}-\varphi$

$$\boldsymbol{\mathcal{E}}(t)=\boldsymbol{\mathcal{E}}_0(t)\cos(\omega t-\phi). \tag{7}$$

The term in Eq. (1) that is proportional to the identity operator I only causes an energy offset but no observable evolution and will therefore be discarded, as commonly done in NMR.

The coupling to a resonant field can be described by an effective Hamiltonian obtained by invoking the rotating wave approximation (RWA) (compare with Appendix B),

$$\mathsf{H}_{\text{eff}}^\alpha=\frac{1}{2}(\omega_\alpha-\omega)[\mathsf{B}_\alpha^\dagger,\mathsf{B}_\alpha]+\frac{\omega_1}{2}(\mathsf{B}_\alpha^\dagger e^{i\phi}+\mathsf{B}_\alpha e^{-i\phi}), \tag{8}$$

where $\omega_1\equiv\boldsymbol{\mu}^{ab}\cdot\boldsymbol{\mathcal{E}}_0$ is the Rabi frequency.[25,26] Due to the RWA only the transition dipole moments are included in the coupling to the field and contributions from permanent dipoles are discarded. Note that in the $\mathbf{k}=0$ limit

$$\mathsf{B}^\dagger e^{i\phi}+\mathsf{B}e^{-i\phi}=\mathsf{B}^\dagger e^{-i\varphi}+\mathsf{B}e^{i\varphi}=\begin{cases}(\mathsf{B}^\dagger+\mathsf{B}) & \text{for}\quad \varphi=0\\ -i(\mathsf{B}^\dagger-\mathsf{B}) & \text{for}\quad \varphi=\dfrac{\pi}{2}\\ -(\mathsf{B}^\dagger+\mathsf{B}) & \text{for}\quad \varphi=\pi\\ i(\mathsf{B}^\dagger-\mathsf{B}) & \text{for}\quad \varphi=\dfrac{3\pi}{2}\end{cases}. \tag{9}$$

In NMR, the pulse fields with phases 0, $\pi/2$, π, and $3\pi/2$ are therefore commonly denoted x, y, $\overline{x}$ (or $-x$), and $\overline{y}$ (or $-y$) pulses, respectively. This convention becomes clear when the Hamiltonian (8) is expressed in Cartesian basis operators,[22]

$$\mathsf{H}_{\text{eff}}^\alpha=(\omega_\alpha-\omega)\mathsf{I}_z^\alpha+\omega_1(\mathsf{I}_x^\alpha\cos\phi-\mathsf{I}_y^\alpha\sin\phi). \tag{10}$$

The full Hamiltonian for a system of coupled two-level systems in an external field is obtained by adding an interaction Hamiltonian:

$$\mathsf{H}_{\text{eff}}=\sum_\alpha\mathsf{H}_{\text{eff}}^\alpha+\sum_{\alpha<\beta}\mathsf{H}_J^{\alpha\beta}. \tag{11}$$

The most general interaction between two two-level systems α and β can be described by a tensor J that couples the vector operators $\vec{\mathsf{I}}_\alpha$ and $\vec{\mathsf{I}}_\beta$,

$$\mathsf{H}_J^{\alpha\beta}=\vec{\mathsf{I}}_\alpha\cdot\mathsf{J}_{\alpha\beta}\cdot\vec{\mathsf{I}}_\beta. \tag{12}$$

The indirect, electron-density mediated, coupling between nuclear spins in a molecule has this general form since the electron density of a molecule is anisotropic. In a liquid, the fast (on the NMR timescale) rotational reorientation of the molecule with respect to the external field averages the tensor J and reduces it to the isotropic indirect coupling in which case the averaged coupling tensor is given by the trace of J times the identity matrix,[1]

$$\mathsf{H}_{J,\text{iso}}^{\alpha\beta}=J_{\alpha\beta}(\mathsf{I}_x^\alpha\mathsf{I}_x^\beta+\mathsf{I}_y^\alpha\mathsf{I}_y^\beta+\mathsf{I}_z^\alpha\mathsf{I}_z^\beta) \tag{13}$$

$$=J_{\alpha\beta}(\mathsf{B}_\alpha^\dagger\mathsf{B}_\beta+\mathsf{B}_\alpha\mathsf{B}_\beta^\dagger+\tfrac{1}{4}[\mathsf{B}_\alpha^\dagger,\mathsf{B}_\alpha][\mathsf{B}_\beta^\dagger,\mathsf{B}_\beta]). \tag{14}$$

The direct magnetic dipole–dipole coupling between two spins is described by a traceless tensor J of rank 1 that averages to zero under fast rotational reorientation. The standard liquid state NMR Hamiltonian therefore contains in addition to the Zeeman term only the indirect isotropic coupling terms. In contrast, the solid state NMR Hamiltonian, where no fast rotational reorientation takes place, is dominated by the direct dipole–dipole interaction since for standard geometries this is several orders of magnitude larger than the indirect couplings.[24]

The NMR product operator formalism is based on the assumption that the J-coupling between the two-level systems is weak, i.e., the transition frequency differences between different spins are large compared to their coupling $|\omega_\alpha-\omega_\beta|\gg|J_{\alpha\beta}|$. In this case the basis of product states, built from the local spin eigenstates of the uncoupled Hamiltonian, is a good approximation to the eigenstates of the coupled Hamiltonian. In this basis the dipole operator and therefore the action of the pulses retains its simple local form.[27] The isotropic coupling of two spins is given by Eq. (13). The terms involving $\mathsf{I}_x^\alpha\mathsf{I}_x^\beta$ and $\mathsf{I}_y^\alpha\mathsf{I}_y^\beta$ yield off-diagonal matrix elements in the Hamiltonian expressed in the product basis. According to perturbation theory to first order in J, these off-diagonal elements can be neglected if the coupling is much smaller than the transition frequency difference, i.e., if the coupling is nonresonant. The general truncated weak J-coupling NMR or optical Hamiltonian for an arbitrary number of spins is then given by Eq. (11) combined with Eq. (8) or (10) and

$$\mathsf{H}_J^{\alpha\beta}=J_{\alpha\beta}\mathsf{I}_z^\alpha\mathsf{I}_z^\beta. \tag{15}$$

Equation (15) can be alternatively rewritten in terms of creation and annihilation operators as follows

$$\mathsf{H}_J^{\alpha\beta}=\frac{J_{\alpha\beta}}{4}[\mathsf{B}_\alpha^\dagger,\mathsf{B}_\alpha][\mathsf{B}_\beta^\dagger,\mathsf{B}_\beta]. \tag{16}$$

This Hamiltonian forms the basis for the model calculations in the remainder of the paper. We shall also need the Hamiltonian for the free evolution between pulses. Using the same approximations we have

$$\mathsf{H}_0=\sum_\alpha \omega_\alpha \mathsf{I}_z^\alpha+\sum_{\alpha<\beta} J_{\alpha\beta}\mathsf{I}_z^\alpha \mathsf{I}_z^\beta \equiv \mathsf{H}_Z+\mathsf{H}_J, \tag{17}$$

or using creation/annihilation operators

$$\mathsf{H}_0=\sum_\alpha \frac{\omega_\alpha}{2}[\mathsf{B}_\alpha^\dagger,\mathsf{B}_\alpha]+\sum_{\alpha<\beta}\frac{J_{\alpha\beta}}{4}[\mathsf{B}_\alpha^\dagger,\mathsf{B}_\alpha][\mathsf{B}_\beta^\dagger,\mathsf{B}_\beta]. \tag{18}$$

In this model the coupling Hamiltonian H_J commutes with the Zeeman Hamiltonian H_Z. This simplifies the calculations and analysis.

III. PRODUCT OPERATOR FORMALISM FOR WEAK OPTICAL FIELDS

In this section we will derive a description of optical spectroscopy of two-level systems subject to weak pulses in close analogy to the POF of NMR. We will only consider nonoverlapping pulses which is the common case in NMR and enforce a time-ordering of the interactions of the system with the electromagnetic fields. A zero delay therefore does not refer to overlapping pulses but to two distinct pulses (ideally rectangular) with a time delay that is very short compared to any evolution of the system. In NMR this is commonly referred to as *composite pulses*. For weakly *J*-coupled two-level systems the free evolution of the system between pulses is the same as in the POF and the formalism will thus allow us to describe the evolution of the density matrix analytically, like in liquid state NMR.

The evolution of the density matrix ρ is given by the Liouville–von Neumann equation

$$\dot{\rho}_t=-i[\mathsf{H}_t,\rho_t]-\mathbf{\Gamma}\rho_t, \tag{19}$$

where the time-dependent Hamiltonian $\mathsf{H}_t=\mathsf{H}_0+\mathsf{V}_t$ can be separated into the unperturbed part H_0 [e.g., the Hamiltonian of Eq. (17)] and the interaction with the electromagnetic field $\mathsf{V}_t=-\boldsymbol{\mu}\cdot\boldsymbol{\mathcal{E}}(\mathbf{r},t)$. The relaxation superoperator $\mathbf{\Gamma}$ will be neglected in most of the following discussion. The corresponding Liouville operators are defined as

$$\mathcal{L}_0\rho=[\mathsf{H}_0,\rho]-i\mathbf{\Gamma}\rho, \quad \mathcal{V}_t\rho=[\mathsf{V}_t,\rho], \quad \mathcal{L}_t=\mathcal{L}_0+\mathcal{V}_t. \tag{20}$$

The formal solution of the Liouville–von Neumann equation for a sequence of n well separated pulses of duration $\tilde{\tau}_j$ and with delays τ_j $(j=1,\ldots,n)$ can be written as

$$\rho_t=\mathcal{G}_0(\tau_n)\mathcal{G}_p(\tilde{\tau}_n)\mathcal{G}_0(\tau_{n-1}) \times\mathcal{G}_p(\tilde{\tau}_{n-1})\cdots\mathcal{G}_0(\tau_2)\mathcal{G}_p(\tilde{\tau}_2)\mathcal{G}_0(\tau_1)\mathcal{G}_p(\tilde{\tau}_1)\rho_0, \tag{21}$$

where τ_n is the time after the end of the last pulse and $t_n=\sum_{j=1}^{n-1}(\tau_j+\tilde{\tau}_j)$ which gives $t=t_{n+1}$. The propagators (Green's functions) are given by

$$\mathcal{G}_p(\tilde{\tau}_j)=\exp_+\left(-i\int_{t_j}^{t_j+\tilde{\tau}_j}\mathcal{L}_t dt\right)$$

and

$$\mathcal{G}_0(\tau_j)=\exp(-i\mathcal{L}_0\tau_j), \tag{22}$$

where $\exp_+$ refers to the positive time ordered exponential operator.[13]

We further decompose the total field $\boldsymbol{\mathcal{E}}(\mathbf{r},t)$ into a sum of fields representing the individual pulses.

$$\boldsymbol{\mathcal{E}}(t)=\sum_j \boldsymbol{\mathcal{E}}_j(t-t_j)\exp[-i(\omega_j t-\phi_j)] +\boldsymbol{\mathcal{E}}_j^*(t-t_j)\exp[i(\omega_j t-\phi_j)]. \tag{23}$$

The jth pulse field in the sum is determined by its envelope $\mathcal{E}_j(t)$ and polarization (note that $\boldsymbol{\mathcal{E}}_j$ is a vector), its frequency ω_j and the phase $\phi_j=\mathbf{k}_j\cdot\mathbf{r}-\varphi_j$ that consists of the spatial contribution $\mathbf{k}_j\cdot\mathbf{r}$ ($\mathbf{k}_j$ being the wave vector) and an additional arbitrary controllable phase φ_j.[20,28] The jth field is nonzero only during the interval from t_j to $t_j+\tilde{\tau}_j$ and we can therefore also decompose V_t in sums over the contributions of the individual pulses,

$$\mathsf{V}_t=\sum_j \mathsf{V}_j=\sum_j -\boldsymbol{\mu}\cdot\boldsymbol{\mathcal{E}}_j(t-t_j)\exp(-i(\omega_j t-\phi_j)) -\boldsymbol{\mu}\cdot\boldsymbol{\mathcal{E}}_j^*(t-t_j)\exp(i(\omega_j t-\phi_j)). \tag{24}$$

The Liouville operator $\mathcal{V}_t$ can be decomposed analogously with $\mathcal{V}_j\rho=[\mathsf{V}_j,\rho]$. The treatment of the free evolution $\mathcal{G}_0$ during the delay periods τ_j between the pulses is identical for NMR and optical spectroscopy but differences between the two arise from several facts.[20,29] The equilibrium density matrix (initial condition) ρ_0 is given by the high temperature approximation in NMR while in optical spectroscopy it will either contain only the global ground state of the system (zero temperature) or be even more complicated based on the eigenvalues of the Hamiltonian H_0. More important are the differences in the treatment of the pulse propagation operators $\mathcal{G}_p(\tilde{\tau}_j)$. In NMR the field wavelength is much longer than the sample size and therefore there are no phase-matching conditions that have to be fulfilled. This is in contrast to optical spectroscopy where phase-matching yields directional responses. NMR therefore effectively corresponds to the $\mathbf{k}=0$ limit. The other important difference is that NMR is a strong field spectroscopy while optical spectroscopy is typically carried out in the weak field regime.

It is convenient to treat the pulse propagation operators $\mathcal{G}_p(\tilde{\tau}_j)$ as effective mappings $\mathcal{G}_{p_j}:\rho_{t_j}\rightarrow\rho_{t_j+\tilde{\tau}_j}$ without explicitly stating their time-dependent nature and then to keep only the time variables τ_j for the description of the experiment. In the strong field limit in NMR this is possible since one can neglect the free evolution due to $\mathcal{L}_0$ during the pulse, as long as all eigenvalues of H_0 (in the rotating frame, i.e., the offsets from the pulse frequency) are small compared to the Rabi frequency. This yields the well known expressions describing pulses as finite rotations in spin space with phase ϕ and flip-angle θ.[1,19] The general transformation rules are summarized in Table I. In the weak field limit the free evolution can be discarded during the pulse either for similar reasons as in NMR or if the duration of the pulse is short compared to the frequency detuning from resonance. The

TABLE I. Pulse transformation rules for spin-$\frac{1}{2}$ systems in the NMR product operator formalism. The angles θ and φ denote the flip angle and pulse phase (in the x-y plane), respectively.

Operator	$\xrightarrow{(\theta)_\varphi}$
I_x	$(\cos^2\varphi+\sin^2\varphi\cos\theta)\,\mathsf{I}_x+\cos\varphi\sin\varphi(1-\cos\theta)\,\mathsf{I}_y-\sin\varphi\sin\theta\mathsf{I}_z$
I_y	$\cos\varphi\sin\varphi(1-\cos\theta)\,\mathsf{I}_x+(\sin^2\varphi+\cos^2\varphi\cos\theta)\,\mathsf{I}_y+\cos\varphi\sin\theta\mathsf{I}_z$
I_z	$\sin\varphi\sin\theta\,\mathsf{I}_x-\cos\varphi\sin\theta\,\mathsf{I}_y+\cos\theta\,\mathsf{I}_z$

exponential function in $\mathcal{G}_p(\tilde{\tau}_j)$ can then be expanded to first order in the field, yielding the formal expression,

$$\mathcal{G}_{p_j}\rho \doteq \mathsf{I}\rho - i[\mathsf{V}_j,\rho] = (\mathsf{I} - i\,\mathcal{V}_j)\rho. \tag{25}$$

Here the relaxation caused by $\mathbf{\Gamma}$ is discarded during the pulses. The density matrix prepared by an n-pulse sequence to nth-order in the fields is then given by

$$\rho_t^{(n)} = (-i)^n\,\mathcal{G}_0(\tau_n)\mathcal{V}_n\mathcal{G}_0(\tau_{n-1}) \times \mathcal{V}_{n-1}\cdots\mathcal{G}_0(\tau_2)\mathcal{V}_2\mathcal{G}_0(\tau_1)\mathcal{V}_1\rho_0. \tag{26}$$

The lower order terms may be obtained by systematically substituting $\mathcal{V}$-operators by identity operators I and summing over all terms that then contain the same number of $\mathcal{V}$'s.

The transformations used to describe a pulse sequence are conveniently depicted by arrows in the following way:

$$\rho' = \mathcal{G}_0(\tau)\rho \leftrightarrow \rho \xrightarrow{\mathsf{H}_0\tau} \rho', \tag{27}$$

$$\rho' = \mathcal{G}_p(\tau)\rho \leftrightarrow \rho \xrightarrow{(\theta)_\phi} \rho', \tag{28}$$

$$\rho' = -i\mathcal{V}\rho \leftrightarrow \rho \xrightarrow{\phi^w} \rho'. \tag{29}$$

In addition to the transformation symbols for free evolution $\mathsf{H}_0\tau$ and strong pulses $(\theta)_\phi$, that are generally used in NMR, we have introduced a symbol representing the application of a weak pulse ϕ^w which is characterized by its phase ϕ. The most commonly used pulses in NMR have flip angles $\theta = \pi/2,\pi$ and phases $\phi = 0,\pi/2,\pi,3\pi/2$. The Zeeman and the J-coupling Hamiltonian commute, as noted above, in our weak J-coupling case, making it possible to factorize the free evolution propagator as

$$\mathcal{G}_0(\tau) = \mathcal{G}_Z(\tau)\mathcal{G}_J(\tau) \text{ or } \rho \xrightarrow{\mathsf{H}_J} \rho' \xrightarrow{\mathsf{H}_Z} \rho''. \tag{30}$$

The fact that H_Z and H_J commute also implies that the product basis, which is the eigenbasis of H_Z, is still the eigenbasis of the weak J-coupling Hamiltonian. This simplifies the evaluation of the pulse and evolution propagators considerably. In the case of strong J coupling we can still express the action of pulses by the simple transformation rules in the product basis and then transform ρ to the eigenbasis of H_0 to calculate the evolution due to $\mathcal{G}_0$. The NMR product operator formalism gives transformation rules for all possible terms that constitute the density matrix under the action of $\mathcal{G}_Z$, $\mathcal{G}_J$ and strong pulses, which allows us to calculate the density matrix propagation analytically for an arbitrary NMR experiment.[1,19] We can use the same transformation rules for the free evolution periods in pulsed resonant optical spectroscopy. Yet it is necessary to derive transformation rules for the action of the weak optical pulses. We have to take into account that unlike in NMR the dipoles of the optical transitions are anisotropic and have fixed orientations with respect to the molecular frame. They also vary between different chromophores of the same transition frequency. Another difference is that, as shown in Appendix B, spin systems naturally absorb and emit circularly polarized radiation while in optical spectroscopy linearly polarized light is commonly used. While the discussion so far in this section was more general, we now return to the effective Hamiltonian in Eq. (8), which implies the RWA, to determine the nonzero matrix elements of the operators V_j for resonant spectroscopy:

$$\mathsf{V}_{j,ab} = \tfrac{1}{2}\mathsf{V}^+_{j,ab}e^{i\phi_j} + \tfrac{1}{2}\mathsf{V}^-_{j,ab}e^{-i\phi_j}, \tag{31}$$

where

$$\mathsf{V}^+_{j,ab} = \boldsymbol{\mu}^{ab}\cdot\boldsymbol{\mathcal{E}}_j(\omega_{ab}-\omega_j), \tag{32}$$

$$\mathsf{V}^-_{j,ab} = \boldsymbol{\mu}^{ab}\cdot\boldsymbol{\mathcal{E}}^*_j(\omega_{ab}+\omega_j). \tag{33}$$

Here $\mathcal{E}_j(\omega)\equiv\int dt\mathcal{E}_j(t)\exp(i\omega t)$ denotes the spectral envelope of the jth pulse.[30] The operators V_j can then be expressed in terms of the $\mathsf{B}^\dagger$ and B operators:

$$\mathsf{V}_j = \tfrac{1}{2}(\mathsf{V}^+_{j,ab}e^{i\phi_j}\mathsf{B}^\dagger + \mathsf{V}^-_{j,ab}e^{-i\phi_j}\mathsf{B}), \tag{34}$$

which for $\mathsf{V}^+_{j,ab} = \mathsf{V}^-_{j,ab}$ becomes

$$\mathsf{V}_j = \mathsf{V}_{j,ab}(\mathsf{I}_x\cos\phi_j - \mathsf{I}_y\sin\phi_j) = \tfrac{1}{2}\mathsf{V}_{j,ab}(\mathsf{I}^+e^{i\phi_j} + \mathsf{I}^-e^{-i\phi_j}). \tag{35}$$

The application of a pulse to a I_x component of the density matrix yields therefore,

$$\mathcal{V}_j\mathsf{I}_x \propto -[\mathsf{I}_y,\mathsf{I}_x]\sin\phi_j = i\sin\phi_j\mathsf{I}_z \tag{36}$$

and to a I_y term,

$$\mathcal{V}_j\mathsf{I}_y \propto [\mathsf{I}_x,\mathsf{I}_y]\cos\phi_j = i\cos\phi_j\mathsf{I}_z. \tag{37}$$

These are perturbation theory results for the limiting case of weak fields and are therefore in general different from the rotations found for the strong $\pi/2$-pulses in NMR ($\mathbf{k}=0$, see also Table I), where

$$\mathsf{I}_x \xrightarrow{(\pi/2)_\varphi} \cos^2\varphi\,\mathsf{I}_x + \cos\varphi\sin\varphi\,\mathsf{I}_y - \sin\varphi\,\mathsf{I}_z, \tag{38}$$

$$\mathsf{I}_y \xrightarrow{(\pi/2)_\varphi} \sin^2\varphi\,\mathsf{I}_y + \cos\varphi\sin\varphi\,\mathsf{I}_x + \cos\varphi\,\mathsf{I}_z. \tag{39}$$

Keeping in mind that $\phi = \mathbf{k}\cdot\mathbf{r} - \varphi$, which accounts for the change in sign of the $\sin\varphi$ terms, we can see that for the special cases where $\varphi = 0,\pi/2,\pi,3\pi/2$ the transformations due to weak pulses and the NMR $\pi/2$-pulses are closely related. For the weak pulses though, the component that coincides with the rotation axis is mapped to zero in this order of the field, while it is retained for strong pulses in NMR. This is a result of the expansion of the response in orders of the field in Eq. (26). The component parallel to the rotation axis, which is the component that remains in the I_x-I_y plane after the pulse, contributes to the response one order lower in the fields in the perturbative expansion and can be observed in a different phase-matched direction. Since NMR corresponds to the $\mathbf{k}=0$ limit, all these responses are observed

TABLE II. Transformation rules for operators under the action of weak pulses. The full transformation of the density matrix is described by the transformation rules with ϕ^w while the rules with $\phi^{\pm}$ describe the result including macroscopic directional detection (see text).

	I_x	I_y	I_z	I^+	I^-
$\xrightarrow{\phi^w}$	$i\sin\phi\mathsf{I}_z$	$i\cos\phi\mathsf{I}_z$	$-i(\cos\phi\mathsf{I}_y+\sin\phi\mathsf{I}_x)$	$-e^{-i\phi}\mathsf{I}_z$	$e^{i\phi}\mathsf{I}_z$
$\xrightarrow{\phi^+}$	$\frac{1}{2}e^{i\phi}\mathsf{I}_z$	$(i/2)e^{i\phi}\mathsf{I}_z$	$-\frac{1}{2}e^{i\phi}\mathsf{I}^+$	0	$e^{i\phi}\mathsf{I}_z$
$\xrightarrow{\phi^-}$	$-\frac{1}{2}e^{-i\phi}\mathsf{I}_z$	$(i/2)e^{-i\phi}\mathsf{I}_z$	$\frac{1}{2}e^{-i\phi}\mathsf{I}^-$	$-e^{i\phi}\mathsf{I}_z$	0

TABLE III. Pulse transformation rules for two consecutive weak pulses with phases ϕ_j and ϕ_k. With the appropriate phase relationship the result resembles the action of a NMR π pulse (see text and Table I).

Operator	$\xrightarrow{\phi_j^w}\ \xrightarrow{\phi_k^w}$
I_x	$\sin\phi_j(\cos\phi_k\mathsf{I}_y+\sin\phi_k\mathsf{I}_x)$
I_y	$\cos\phi_j(\cos\phi_k\mathsf{I}_y+\sin\phi_k\mathsf{I}_x)$
I_z	$\cos(\phi_j-\phi_k)\mathsf{I}_z$

simultaneously and the POF rules have to account for them. The application of a pulse to an I_z term yields

$$\mathcal{V}_j\mathsf{I}_z\propto[\mathsf{I}_x,\mathsf{I}_z]\cos\phi_j-[\mathsf{I}_y,\mathsf{I}_z]\sin\phi_j = -i(\cos\phi_j\mathsf{I}_y+\sin\phi_j\mathsf{I}_x), \tag{40}$$

which is, apart from the overall factor i, the same result as for a $\pi/2$-pulse in NMR:

$$\mathsf{I}_z\xrightarrow{(\pi/2)_\varphi}-\cos\varphi\mathsf{I}_y+\sin\varphi\mathsf{I}_x. \tag{41}$$

Immediate application of two consecutive pulses gives

$$\begin{aligned}\mathcal{V}_k\mathcal{V}_j\mathsf{I}_z&\propto-i(\cos\phi_j\cos\phi_k[\mathsf{I}_x,\mathsf{I}_y]-\sin\phi_j\sin\phi_k[\mathsf{I}_y,\mathsf{I}_x])\\&=(\cos\phi_j\cos\phi_k+\sin\phi_j\sin\phi_k)\mathsf{I}_z\\&=\cos(\phi_j-\phi_k)\mathsf{I}_z,\end{aligned} \tag{42}$$

which is $-\mathsf{I}_z$ for a phase relationship between the two pulses of $\phi_j-\phi_k=\pi$.

Similarly, the application of two back-to-back pulses to I_x yields

$$\mathcal{V}_k\mathcal{V}_j\mathsf{I}_x\propto i\sin\phi_j\mathcal{V}_k\mathsf{I}_z\propto\sin\phi_j(\cos\phi_k\mathsf{I}_y+\sin\phi_k\mathsf{I}_x) \tag{43}$$

and to I_y

$$\mathcal{V}_k\mathcal{V}_j\mathsf{I}_y\propto i\cos\phi_j\mathcal{V}_k\mathsf{I}_z\propto\cos\phi_j(\cos\phi_k\mathsf{I}_y+\sin\phi_k\mathsf{I}_x). \tag{44}$$

With two phase-controlled pulses it is therefore possible to achieve the simultaneous inversion of I_z and one of I_x, I_y which is the same result as for π_x or π_y-pulses in NMR (compare Tables I and III for $\theta=\pi$). The pulses that form the composite pulse must have a phase difference of π. To invert I_x, the first phase must be $(\pi/2)+k\pi$ while with a pulse phase of $k\pi$ for the first pulse it is possible to invert I_y in addition to I_z. What is different from NMR though is that a π_x-pulse preserves the I_x component and a π_y-pulse the I_y component while the weak composite pulses map these components to zero (in this order).

Note that $\sin\phi$ and $\cos\phi$ contain both the geometric and the pulse phase and therefore:

$$\cos\phi_j=\tfrac{1}{2}(e^{i\mathbf{k}_j\cdot\mathbf{r}}e^{-i\varphi_j}+e^{-i\mathbf{k}_j\cdot\mathbf{r}}e^{i\varphi_j})$$

$$\sin\phi_j=\frac{-i}{2}(e^{i\mathbf{k}_j\cdot\mathbf{r}}e^{-i\varphi_j}-e^{-i\mathbf{k}_j\cdot\mathbf{r}}e^{i\varphi_j}).$$

For a sequence of pulses with wave vectors $\mathbf{k}_1,\mathbf{k}_2,\ldots,\mathbf{k}_n$, the phase-matching conditions yield 2^n signals in the directions given by $\mathbf{k}_S=\Sigma_{i=1}^n\pm\mathbf{k}_j$. For these signals $(\mathbf{k}_S-\Sigma\pm\mathbf{k}_j)\cdot\mathbf{r}=0$ is satisfied for all sites $\mathbf{r}$ in the macroscopic sample. Adding two signals observed in directions that differ by the sign of $\mathbf{k}_j$ of only one pulse therefore gives a signal corresponding to a term with $\cos\phi_j\rightarrow\cos\varphi_j$ and subtraction yields the $\sin\phi_j\rightarrow-\sin\varphi_j$ term. For a single pulse it is possible to get the same result by taking the real or imaginary part of the signal in only one of the directions $+\mathbf{k}$ or $-\mathbf{k}$.

Phase matching and directional detection are macroscopic effects which allow to observe signals related to operators which are not self-adjoined and that could therefore not be microscopic observables. This is completely analogous to the signals observed after phase-cycling or to the use of the operator I^+ as detection operator in NMR.[31] We use the density matrix rather as a tool to describe the outcome of the macroscopic experiment than the microscopic evolution of the system that is studied. It is therefore possible to introduce pulse transformation operators that correspond to observing the signal in only one phase-matched direction,

$$\mathsf{V}_{j,ab}\mathsf{I}^+e^{i\phi_j}\ \text{ and }\ \mathsf{V}_{j,ab}\mathsf{I}^-e^{-i\phi_j}, \tag{45}$$

which we will symbolize by the transformations

$$\rho\xrightarrow{\phi^+}\rho'\ \text{ and }\ \rho\xrightarrow{\phi^-}\rho'. \tag{46}$$

Each of these transformations can be directly related to a sum of two double-sided Feynman diagrams where a field with wave vector $+\mathbf{k}$ $(-\mathbf{k})$ interacts with either the bra or the ket of the density matrix element.

All transformation rules necessary to describe a weak-pulse experiment are given in Table II. We can summarize them in a similar fashion as in the diagrams used for the product operator formalism (see e.g., Ref. 1 Fig. 2.1.4). The I_z evolution and the coupling transformations are identical to the POF and describe the evolution under $\mathcal{G}_0(\tau)$ during the delay times. Since we can generate terms in the density matrix expansion that contain I^+ or I^- by applying the phase matched ϕ^+ and ϕ^- pulses, we also need to know the transformation rules for I^+ and I^- for free evolution ($\alpha=x$, y, or z):

$$\mathsf{I}_k^{\pm}\xrightarrow{\phi\mathsf{I}_z^k}\mathsf{I}_k^{\pm}e^{\mp i\phi}, \tag{47}$$

$$\mathsf{I}_k^{\pm}\xrightarrow{\phi 2\mathsf{I}_z^k\mathsf{I}_\alpha^l}\mathsf{I}_k^{\pm}\cos\phi\mp i\,2\mathsf{I}_k^{\pm}\mathsf{I}_\alpha^l\sin\phi, \tag{48}$$

$$\mathsf{I}_k^{\pm}\xrightarrow{\phi 2\mathsf{I}_x^k\mathsf{I}_\alpha^l}\mathsf{I}_k^{\pm}\cos^2\frac{\phi}{2}+\mathsf{I}_k^{\mp}\sin^2\frac{\phi}{2}\pm i\mathsf{I}_z^k\mathsf{I}_\alpha^l\sin\phi, \tag{49}$$

$$\mathsf{I}_k^{\pm} \xrightarrow{\phi 2\mathsf{I}_y^k \mathsf{I}_\alpha^l} \mathsf{I}_k^{\pm} \cos^2\frac{\phi}{2} - \mathsf{I}_k^{\mp} \sin^2\frac{\phi}{2} - 2\mathsf{I}_z^k \mathsf{I}_\alpha^l \sin\phi. \tag{50}$$

These rules are rarely used in the POF for the description of NMR experiments since pulses that produce $\mathsf{I}^{\pm}$ terms are not directly available without directional detection. The diagrams for x- and y-pulses differ from the ones in the POF. Since we treat the weak field limit to first order we effectively obtain the derivative operators. The possible flip angles are the two orthogonal cases of $\theta=0$ and $\pi/2$, while in NMR any finite flip angle can be achieved. $\theta=0$ corresponds to no interaction with the field and contributes to the response one order lower in the field. The operators that are constant under the NMR pulse transformations are mapped to zero in a given order, i.e., x-pulses transform $\mathsf{I}_z \rightarrow -\mathsf{I}_y \rightarrow -\mathsf{I}_z \rightarrow \mathsf{I}_y \rightarrow \mathsf{I}_z$ and map I_x to zero and y-pulses transform $\mathsf{I}_z \rightarrow \mathsf{I}_x \rightarrow -\mathsf{I}_z \rightarrow -\mathsf{I}_x \rightarrow \mathsf{I}_z$ and map I_y to zero.

The application of a pulse P simultaneously to two (or more) two-level systems is described in NMR by the application of the transformation operators to the individual components in the direct product, i.e.:

$$\mathsf{P}(\mathsf{I}_\alpha \otimes \mathsf{I}_\beta) = \mathsf{P}\mathsf{I}_\alpha \otimes \mathsf{P}\mathsf{I}_\beta. \tag{51}$$

In the weak field limit pulses act on products of operators according to the Leibniz rule (product rule), i.e.,

$$\mathsf{P}(\mathsf{I}_\alpha \otimes \mathsf{I}_\beta) = \mathsf{P}\mathsf{I}_\alpha \otimes \mathsf{I}_\beta + \mathsf{I}_\alpha \otimes \mathsf{P}\mathsf{I}_\beta, \tag{52}$$

which is the mathematical property of a derivation operator. This formally expresses the fact that in the weak field limit the coherence order can only change by ± 1.

In summary, the general procedure for the calculation of the effect of a pulse sequence on a density matrix consists of the following steps:

1. In the low temperature limit start with $\rho_0 = \Pi_\alpha(\mathsf{I}^\alpha - \mathsf{I}_z^\alpha)$.
2. Apply alternatingly pulse propagators and free propagators.
   - Apply the pulses according to the rules in Table II, keeping the terms containing the phases ϕ for bookkeeping.
   - The free evolution under $\mathcal{G}_0(\tau)$ during the delays τ can be obtained analytically in the weak J-coupling limit using the rules of the NMR product operator formalism.
3. In the final expression substitute $\phi = \mathbf{k}\cdot\mathbf{r} - \varphi$ to see which directional signals have to be added with the respective prefactors to obtain results corresponding to x- or y-pulses or which directional signals are discarded to simplify the spectra by coherence pathway selection.
4. Substitute the appropriate phases φ for phase-cycling, composite pulses, etc.

Once the density matrix has been calculated, the nth-order signal can be computed as its trace with the dipole operator,

$$P^{(n)} = \mathrm{tr}\{\boldsymbol{\mu}\rho^{(n)}\} \quad \text{where} \quad \boldsymbol{\mu} = \sum_\alpha \boldsymbol{\mu}_\alpha^{ab}\mathsf{B}_\alpha + \boldsymbol{\mu}_\alpha^{ba}\mathsf{B}_\alpha^\dagger. \tag{53}$$

As an example for these transformation rules, let us consider the photon echo (PE) technique[32] for a single two level system:

$$\begin{aligned}
\rho_0 = \mathsf{I}_z &\xrightarrow{\phi_1^-} \tfrac{1}{2}e^{-i\phi_1}\mathsf{I}^- \\
&\xrightarrow{\mathsf{H}Z\tau_1} \tfrac{1}{2}e^{i(\omega\tau_1-\phi_1)}\mathsf{I}^- \\
&\xrightarrow{\phi_2^+} \tfrac{1}{2}e^{i(\omega\tau_1-\phi_1+\phi_2)}\mathsf{I}_z \\
&\xrightarrow{\phi_3^+} -\tfrac{1}{4}e^{i(\omega\tau_1-\phi_1+\phi_2+\phi_3)}\mathsf{I}^+ \\
&\xrightarrow{\mathsf{H}_Z\tau_3} -\tfrac{1}{4}e^{i(\omega(\tau_1-\tau_3)-\phi_1+\phi_2+\phi_3)}\mathsf{I}^+.
\end{aligned} \tag{54}$$

Here we labeled the second delay time τ_3 to indicate that the possible delay between pulses 2 and 3 has been chosen as $\tau_2=0$. The initial density matrix has been simplified to I_z since the term due to I does not yield any observable signal for a single two level system. The trace of Eq. (53) yields the term with a phase combination $-\phi_1+\phi_2+\phi_3$ which represents the PE signal obtained in the phase matched direction $-\mathbf{k}_1+\mathbf{k}_2+\mathbf{k}_3$.

IV. TWO-DIMENSIONAL OPTICAL ANALOGS OF NMR PULSE SEQUENCES

The simple two- and three-pulse strong field experiments are of great importance in liquid state NMR spectroscopy and yield detailed information about weakly J-coupled spin-$\frac{1}{2}$ systems. In the following we will demonstrate how the same type of information can be extracted for optical two-level systems with weak pulses. We first discuss some important properties of the basic 2D NMR techniques. We then apply the general operator formalism presented in Sec. III to three-pulse experiments performed on a system of weakly J-coupled two-level systems. Comparison of the resulting density matrix evolution and responses with the corresponding NMR experiments reveals the close analogies between weak and strong field experiments.

A general two-dimensional NMR experiment contains four distinct blocks: (1) preparation block, (2) evolution period of variable duration τ_1, (3) mixing block, and (4) detection period τ_2. The complex one-dimensional FID signal is detected as a function of τ_2 in a series of experiments in which τ_1 is incremented. This yields a discretized 2D array of data points as a representation of the 2D signal in the two time variables τ_1 and τ_2. A single peak in this spectrum is commonly described[1] by the Fourier transform of a function,

$$\begin{aligned}
p(\tau_1,\tau_2) = c\,(&\Pi(\tau_1)\exp(-(i\omega+\Gamma)\tau_1))\cdot(\Pi(\tau_2) \\
&\times\exp(-(i\omega'+\Gamma')\tau_2)),
\end{aligned} \tag{55}$$

where c is the complex amplitude, ω,ω' are the frequencies with which the coherence evolves during τ_1 and τ_2, Γ,Γ' are the corresponding relaxation rates, and $\Pi(t)$ are window functions (in the simplest case rectangular) that are nonzero only for the times for which the signal is recorded. The two-

dimensional Fourier transformation yields a spectrum as a function of the two corresponding frequency variables Ω_1 and Ω_2.

$$\tilde{p}(\Omega_1,\Omega_2)=c\int_{-\infty}^{\infty}d\tau_2 e^{i\Omega_2\tau_2}\int_{-\infty}^{\infty}d\tau_1 e^{i\Omega_1\tau_1}p(\tau_1,\tau_2). \tag{56}$$

The peak shape of a single two-dimensional peak in this simple case is then given by (not including the effect of the observation windows Π)

$$\begin{aligned}\tilde{p}(\Omega_1,\Omega_2)=&c\,(a(\Omega_1)a'(\Omega_2)-d(\Omega_1)d'(\Omega_2))\\&+i\,(-a(\Omega_1)d'(\Omega_2)-d(\Omega_1)a'(\Omega_2))\end{aligned} \tag{57}$$

with the Lorentzian absorptive and dispersive components

$$a(\Omega_1)=\frac{\Gamma}{(\omega-\Omega_1)^2+\Gamma^2},\quad a'(\Omega_2)=\frac{\Gamma'}{(\omega'-\Omega_2)^2+\Gamma'^2}, \tag{58}$$

$$d(\Omega_1)=\frac{\Omega_1-\omega}{(\omega-\Omega_1)^2+\Gamma^2},\quad d'(\Omega_2)=\frac{\Omega_2-\omega'}{(\omega'-\Omega_2)^2+\Gamma'^2}. \tag{59}$$

An appropriate choice of the detection phase (or an overall phase correction in the data processing step) allows to select either the real or the imaginary part of the complex signal $\tilde{p}/c$ in Eq. (57). The real part, which corresponds to the real part of the spectrum for a real amplitude c, contains mixed phase peaks which consist of the sum of a pure absorptive and a pure dispersive signal. The absorptive part gives the maximum spectral resolution[1] since the peaks are well localized. With a correctly designed pulse sequence and appropriate 2D data processing[1] it is possible to obtain pure 2D absorptive spectra experimentally. It is therefore highly advantageous to measure the full complex spectrum and not only the absolute value signal. Intermediate relaxation regimes which do not yield a simple exponential decay of the signal as in NMR will result in more complicated two-dimensional peak shapes.[4]

A. NMR two-pulse techniques

In the simplest case, the preparation and mixing blocks consist of only one pulse each, yielding a basic NMR two-pulse echo sequence $(\pi/2)-\tau_1-(\pi)-\tau_2$ [Fig. 1(c)] and the COSY (correlation spectroscopy) sequence $(\pi/2)-\tau_1-(\beta)-\tau_2$ [flip angle $\beta<\pi$, Fig. 1(a)]. Here the phases of the pulses (usually indicated as a subscript to the flip angles in brackets) have been omitted since only the relative phases within the pulse sequence matter and can, in the simplest case, all be chosen to be the same as the phase of the first pulse. In more sophisticated schemes, the phases of the first and second pulse are systematically changed in consecutive experiments and the resulting spectra are added to select specific coherence transfer pathways (phase-cycling, see below). Sometimes it is profitable to place the mixing pulse in the evolution period which gives essentially the same technique but changes the way the spectra are displayed. This *delayed acquisition* converts the basic methods into the well-known J-resolved spectroscopy (JRS) $(\pi/2)-\tau_1/2-(\pi)-\tau_1/2-\tau_2$ and SECSY (spin echo correlation spectroscopy) $(\pi/2)-\tau_1/2-(\beta)-\tau_1/2-\tau_2$, respectively.

COSY is the basic 2D correlation spectroscopy technique and employs a single mixing pulse with rotation angle β to induce coherence transfer. The evolution during τ_1 as well as τ_2 depends on both transition frequencies and couplings, giving rise to complicated multiplet patterns in both Ω_1 and Ω_2. The coherence transfer yields off-diagonal peaks between multiplets that correspond to coupled spins. This allows the identification of coupled spins and the interpretation of the observed coupling multiplets. The resulting peak pattern for a weakly J-coupled two-spin model system is shown in Fig. 1(a). SECSY contains the same information as COSY and differs from it only by the delayed acquisition which starts at the top of the coherence transfer echo. This can be of practical importance in systems that contain groups of chromophores with large differences in their transition frequencies without couplings between the groups. The conventional correlation sequences then lead to 2D spectra where the cross-peaks lie within a narrow band along the diagonal and it is possible to reduce the spectral width in the Ω_1 domain by delaying the acquisition, similar to the case shown in Fig. 1(b).[1] JRS is the simplest example of a two-dimensional NMR technique for the separation of interactions. The central π mixing-pulse refocuses the evolution due to the Zeeman term at the end of time τ_1. The effective evolution during τ_1 is therefore only due to the coupling term in H_0. After 2D Fourier transformation, the spectrum depends only on the couplings in the Ω_1-domain and on frequencies and couplings in the Ω_2-domain, which yields a skew spectrum. The resulting peak pattern for a weakly J-coupled two-spin model system is shown in Fig. 1(b). An additional skew transformation $(\Omega_1'=\Omega_1,\ \Omega_2'=\Omega_2-\Omega_1)$ results in a 2D spectrum that only contains couplings in Ω_1 and frequencies in Ω_2.

All of these pulse sequences can be performed in either a homonuclear (one-color) or heteronuclear (two-color) fashion. Here the term homonuclear describes a system consisting of spins with transition frequencies that are all covered by the pulse bandwidth and therefore all excited unselectively by the pulse. In a heteronuclear system it is possible to selectively excite one kind of spins at one frequency and the other kind at their transition frequency which is well separated. In the heteronuclear mode of these experiments the first pulse is applied to only one kind of spins while the second pulse is applied simultaneously at both frequencies.

B. Optical three-pulse analogs of 2D NMR techniques

As we will discuss next, there are no direct analogs of the simple two-pulse 2D NMR experiments in weak field spectroscopy due to the differences in the coherence transfers achievable by weak and strong field spectroscopy. It is possible though to compare NMR three-pulse experiments that are extensions of the basic two-pulse schemes with corresponding optical experiments.

In the following we consider two weakly coupled two-level systems with the model Hamiltonian of Eq. (17) to

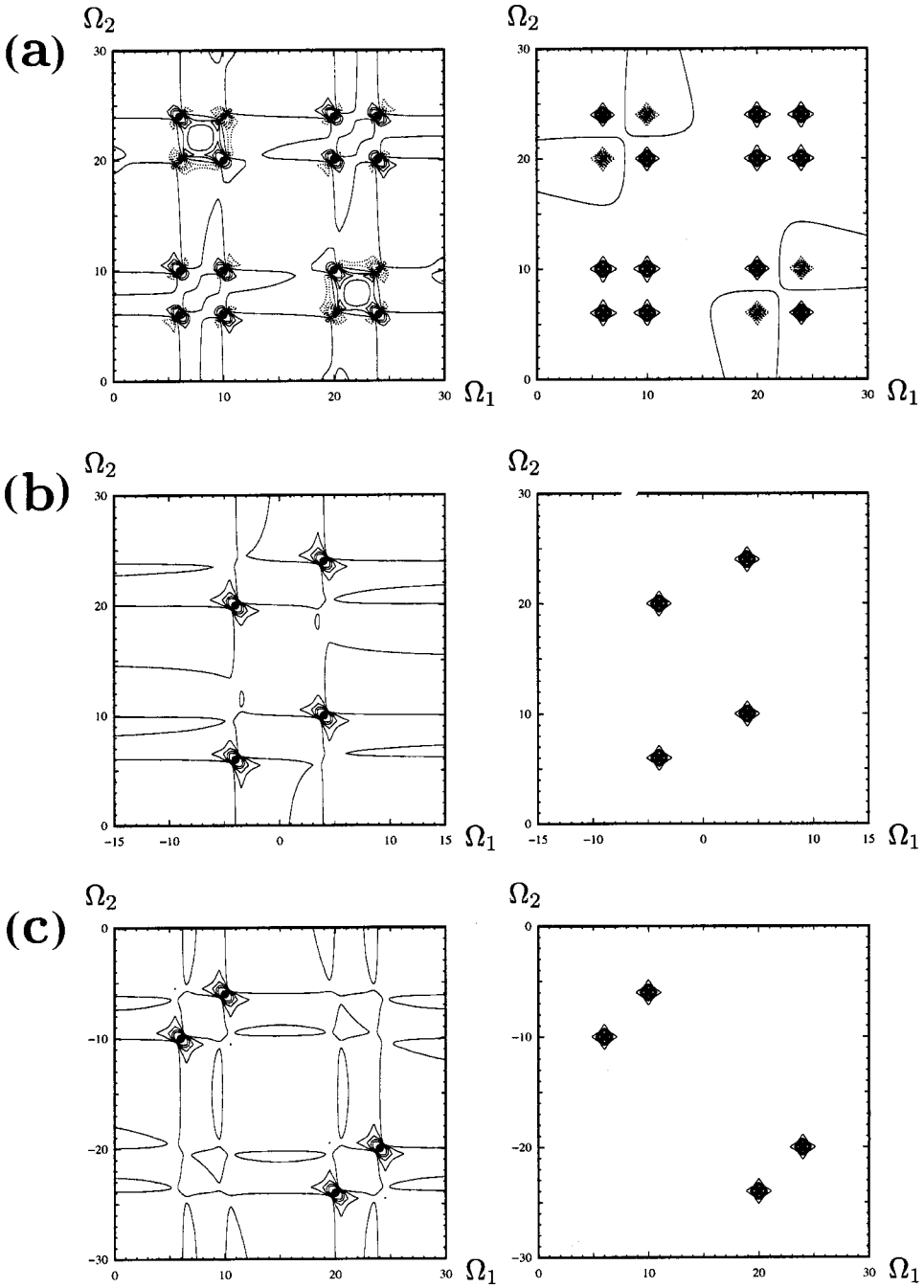

FIG. 1. Spectra of two-pulse NMR techniques for a model system of two weakly J-coupled spins α and β. The transition frequencies are chosen as $\omega_\alpha=8$ and $\omega_\beta=22$ and the coupling is $J=4$ in arbitrary units. In the right column only the absorptive contributions are shown for clarity. Solid contour lines represent a positive signal while negative contours are dotted. (a) COSY spectrum with a $\pi/2$ mixing pulse. The spectrum contains diagonal peaks at $(\omega_\alpha \pm J/2,\omega_\alpha \pm J/2)$ and $(\omega_\beta \pm J/2,\omega_\beta \pm J/2)$ and cross-peaks at $(\omega_\alpha \pm J/2,\omega_\beta \pm J/2)$ and $(\omega_\beta \pm J/2,\omega_\alpha \pm J/2)$. (b) J-resolved spectrum. The spectrum contains peaks at $(-J/2,\omega_{\alpha,\beta}-J/2)$ and $(+J/2,\omega_{\alpha,\beta}+J/2)$. (c) Spectra for the same technique but without delayed acquisition giving rise to peaks along the diagonal. These spectra are closely related to the COSY spectra in the first row but here the mixing pulse has a flip angle π.

identify the closest optical analogs of the basic three-pulse 2D NMR experiments. The energy level scheme for this model including the transition frequencies is given in Fig. 2. The energies corresponding to the levels are $-\Omega+J/4$, $-\Delta-J/4$, $\Delta-J/4$, and $\Omega+J/4$, where $\Omega=(\omega_\alpha+\omega_\beta)/2$ and $\Delta=(\omega_\alpha-\omega_\beta)/2$ and $\omega_\alpha,\omega_\beta$ are the chromophore transition frequencies and J is the weak coupling. The lowest energy is the ground state g, followed by two singly excited states e,e′ and the highest energy is the doubly excited state f. The energy difference between ground state g and doubly excited state f is 2Ω and between the single excited states 2Δ. A model system that is comparable to a weakly coupled two spin system has to fulfill further requirements. The homogeneous linewidths should be small enough so the couplings can be resolved and the coupling needs to be small compared to the difference in transition frequency.

A convenient way of comparing optical and NMR pulse sequences is in terms of their coherence order pathway diagrams. The coherence order of a product operator in the density matrix expansion can be determined by its decomposition in I^+ and I^- operators and is given by the difference between the number of I^+ and the number of I^- occurring in the decomposition.[1] The coherence order of terms in the Feynman diagrams describing single Liouville space pathways can be easily determined as the difference between the excitation number (in terms of the eigenstates of the coupled Hamiltonian) of the ket- and the bra-state. An n quantum coherence is characterized by the fact that it acquires an

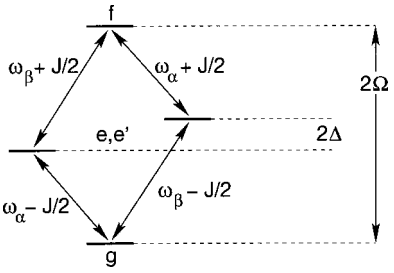

FIG. 2. Energy level scheme for a model system of two weakly J-coupled two-level systems α and β with transition frequencies $\omega_\alpha, \omega_\beta$ and coupling J.

overall phase factor of $\exp(-in\varphi)$ under rotation with an angle φ about the z-axis. This property makes it possible to separate different orders by the use of phase-shifted pulses and forms the basis of *phase-cycling* techniques.[1]

The application of a weak pulse can only change the coherence order by ± 1. In the operator formalism this follows from the fact that the action of a pulse is distributed over a product operator according to the ''product rule'' in Eq. (52). In the resulting sum of product operators each term differs in exactly one place from the product operator before the pulse, yielding a change in coherence order of ± 1. This is different from NMR, where strong pulses can give rise to terms where the coherence order changes by any of the values $0, \pm 1, \pm 2, \ldots$ depending on the product operator before the pulse. Evolution during the pulse without a change in coherence order in NMR can occur for two different reasons, either the pulse has a finite flip angle which is different from $\pi/2$ and some part of the product operator remains untransformed, or the product operator coincides with the rotation axis of the pulse transformation. *For weak pulses any signal that is due to the interaction with a pulse and is observed in a phase matched direction looks like the interaction with a* $\pi/2$ *pulse* and the operator that coincides with the rotation axis of this apparent $\pi/2$ pulse is mapped to zero. This also rules out coherence order changes of zero for weak pulse sequences. If we want to translate coherence order pathway diagrams from NMR to optical spectroscopy, we thus have to retain only the pathways with changes of ± 1 and drop all other pathways.

For the same reasons, the application of two weak pulses can only result in zero quantum and double quantum terms and does not yield any observable signal. This changes if the pulses have a finite flip angle or if we include diagonal elements of the dipole operator. The simplest possible two-dimensional optical experiments thus consist of three pulses where one of the delays τ_1 or τ_2 can be either attributed to the preparation or the mixing block and the remaining two delays τ_2 or τ_1 and τ_3 give, after Fourier transformation, the two frequency domains.

The general third-order responses (see Appendix C) for the three-pulse experiments were obtained using a Maple implementation of the operator formalism expressions given in Sec. III. Collecting the terms with a common overall phase factor yields the directional responses which can be compared to the Feynman-diagrams given in Fig. 3. In the present model of two coupled two-level systems all states are given in the level scheme of Fig. 2. In total there are 2^3 possible Liouville-space pathways. The two pathways with and $\pm(\mathbf{k}_1+\mathbf{k}_2+\mathbf{k}_3)$ do not yield an observable signal for the current model and are therefore not given. The remaining six pathways can be classified as either containing only one negative or only one positive wave vector. We will label the pathways with only one negative wave vector S_{I}, S_{II}, and S_{III}, depending on whether the first, second, or third wave vector has the negative sign and the remaining pathways with only one positive wavevector are S'_{I}, S'_{II}, and S'_{III}, analogously. The expressions for S_{I}, S_{II}, and S_{III} are given in Appendix C and S'_{I}, S'_{II}, and S'_{III} are given by the complex conjugate expressions. *In the examples discussed below we show how these elementary signals can be combined in various ways to achieve a particular goal of 2D NMR.* In NMR these signals are not separated spatially but they can be distinguished by their different dependence on the phase of the field.

The resulting absorptive part of the two-dimensional spectra for very short τ_2 are displayed in Fig. 4 assuming Lorentzian signals of finite linewidth [Eq. (58) with $\Gamma=\Gamma'=1$]. For a simpler comparison with the NMR results, all interaction matrix elements $\mathsf{V}^-_{k,\gamma}$ and $\mathsf{V}^+_{k,\gamma}$ are taken to be equal. In NMR this is automatically fulfilled for spins of the same nuclear species since they all share a common gyromagnetic ratio and all dipoles are oriented in the same direction given by the external static magnetic field. The transition dipoles for the optical transitions have a fixed orientation with respect to the molecular frame and can be oriented arbitrarily with respect to the external field. The size of the transition dipoles can furthermore vary for nonidentical chromophores which are of the same type. Transitions with a frequency that lies within the excitation bandwidth (''homonuclear'' in NMR) can therefore couple to the field with different strengths giving rise to peak intensities that differ. If two transitions are separated by more than the excitation bandwidth of the pulse (''heteronuclear'') the pulses that are applied at the different frequencies might be calibrated to obtain equal transition moments. In addition it is possible to adjust the polarization direction.

The most obvious difference between the optical and the NMR spectra is that in the Ω_1 domain the NMR spectrum contains peaks at $\omega_{\alpha,\beta}\pm J/2$ while the optical spectra only contain peaks at $\omega_{\alpha,\beta}-J/2$. This is due to the different initial density matrices. In the NMR high temperature approximation all levels of the level scheme (Fig. 2) are initially populated and therefore coherences with all possible frequencies can be generated during τ_1 while in the optical low-temperature approximation only the ground state is populated and after the first pulse only coherences involving the ground state will evolve (see also Fig. 3).

C. COSY

Apart from the difference in multiplicity along Ω_1, the spectrum corresponding to the technique S_{III}, where τ_2 is fixed, is the closest analog to COSY (see Fig. 5) since the mixing sequence consisting of pulses two and three correlates the coherences between any excited state and the

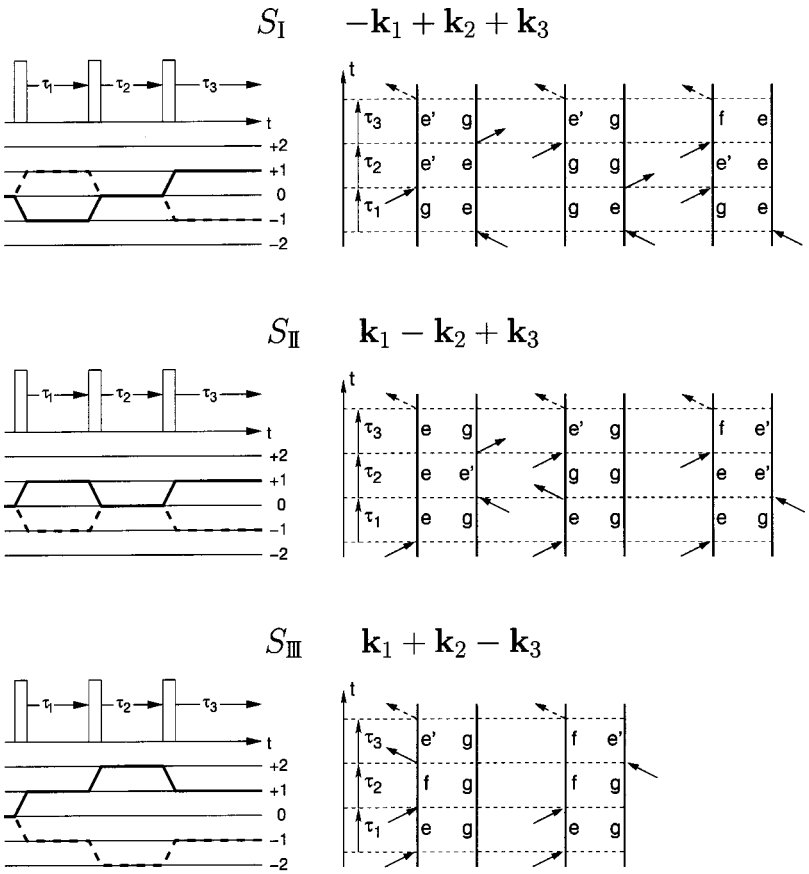

FIG. 3. Feynman diagrams for three-pulse experiments with non-overlapping pulses for the possible signals $S_{\mathrm{I,II,III}}$ (right column) and the corresponding coherence transfer pathways (left column). The dashed lines in the coherence transfer pathway diagrams belong to the signals $S'_{\mathrm{I,II,III}}$.

ground state that exist during τ_1 with all possible coherences between either the ground or the second excited state and the two single excited states which evolve during τ_3. This is exactly the idea of the COSY technique. A comparison of the coherence transfer pathways shows that S_{III} is essentially the double quantum filtered version of the basic COSY experiment which is described by the NMR pulse sequence $(\pi/2)-\tau_1-(\pi/2)-\tau_m-(\pi/2)-\tau_2$. In NMR all responses $S_{\mathrm{I,II,III}}$ and $S'_{\mathrm{I,II,III}}$ would contribute to the signal and lead to dominating diagonal peaks from, e.g., S_{II}, even for uncoupled spins. Double quantum filtering is a phase-cycling technique that suppresses all $S_{\mathrm{I,II}}$ contributions which simplifies the spectra considerably. In the optical case phase cycling is not necessary since it is possible to obtain the same signal from directional detection. We can therefore identify

$$S_{\mathrm{COSY}}(\tau_1,\tau_3)=S_{\mathrm{III}}(\tau_1,\tau_m,\tau_3), \tag{60}$$

where the two time domains are given by τ_1 and τ_3 while $\tau_2=\tau_m$ is a constant delay.

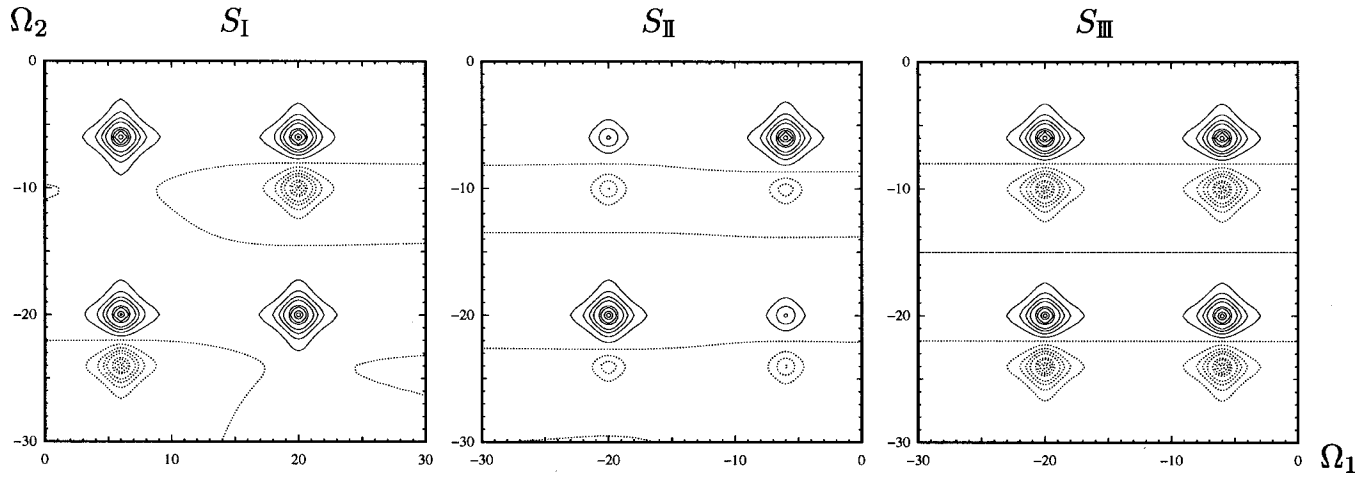

FIG. 4. Pure absorptive part of the two-dimensional spectra corresponding to the responses S_{I}, S_{II}, and S_{III} for small τ_2 (see also Appendix C). Solid contour lines represent a positive signal while negative contours are dotted.

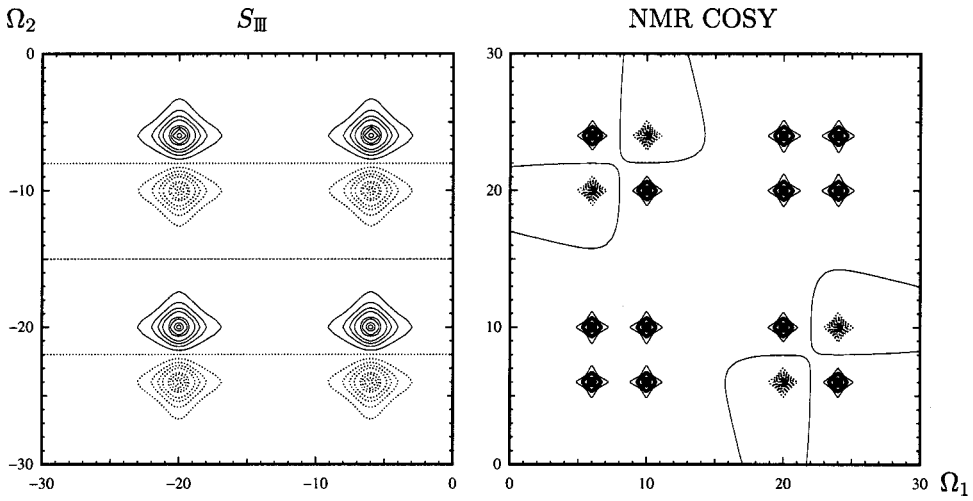

FIG. 5. Comparison of the spectrum from the optical analog of COSY spectroscopy (left) with the NMR COSY spectrum (right) for the same model system. The difference in multiplicity along Ω_1 due to the different initial condition is clearly visible (see text). Solid contour lines represent a positive signal while negative contours are dotted.

D. NOESY and EXSY

The combined responses $S_{\rm I}+S_{\rm II}$ together correspond to NOESY where again the second and third pulse constitute the mixing sequence. The signal is frequency labeled by the evolution of the one quantum coherences (1QC) in τ_1 and τ_3, and cross-peaks appear between chromophores that exhibit cross-relaxation or transport during τ_2. We can therefore identify

$$S_{\rm NOESY}(\tau_1,\tau_3)=S_{\rm I}(\tau_1,\tau_m,\tau_3)+S_{\rm II}(\tau_1,\tau_m,\tau_3). \qquad (61)$$

In NOESY the cross-peaks of interest for determining distances are due to polarization transfer by the Nuclear Overhauser Effect (dipolar cross-relaxation) during τ_m. In 1D spectroscopy the NOE is visible as changes in peak intensity when one of the nuclei is excited by strong irradiation. The detection of these intensity changes is far less sensitive than the observation of a cross-peak in 2D spectroscopy. EXSY is the same technique as NOESY except that the observed evolution during $\tau_m=\tau_2$ is due to chemical exchange rather than cross-relaxation.

The spectra shown in Fig. 4 are for $\tau_2=0$ and without cross-relaxation. The cross-peaks in this case are due to the weak coupling and are considered an unwanted artifact in EXSY or NOESY (“*J cross-peaks*”[1]).

E. *J*-resolved spectroscopy

In the special case of $\tau_2=0$ the response $S_{\rm I}$ yields an echo signal. The system is in a +1QC during τ_1 and in a -1QC during τ_3 and therefore the diagonal peaks refocus for arbitrary inhomogeneous frequency distributions. This signal is related to the NMR echo sequence which is the basis of *J*-resolved spectroscopy that was shown in Fig. 1(c) (without delayed acquisition). The optical spectrum contains additional peaks that are not cancelled as in NMR due to the different initial conditions and the resulting differences in multiplicity in Ω_1. Directional detection allows us to remedy the situation by combining optical signals from different directions which is impossible in NMR. The combination

$$S_{\rm D}=S_{\rm III}(\Omega_1,\Omega_2)-S_{\rm II}(\Omega_1,\Omega_2) \qquad (62)$$

gives only the diagonal peaks that can be subtracted from $S_{\rm I}$ and yield

$$S_{\rm JRS}=S_{\rm I}(-\Omega_1,\Omega_2)-S_{\rm II}(\Omega_1,\Omega_2)+S_{\rm III}(\Omega_1,\Omega_2), \qquad (63)$$

where only the off-diagonal multiplets are retained. This signal can be considered an analog of *J*-resolved spectroscopy (see Fig. 6), since in one frequency dimension the signal depends only on the transition frequencies while it depends on both frequencies and couplings in the second dimension.

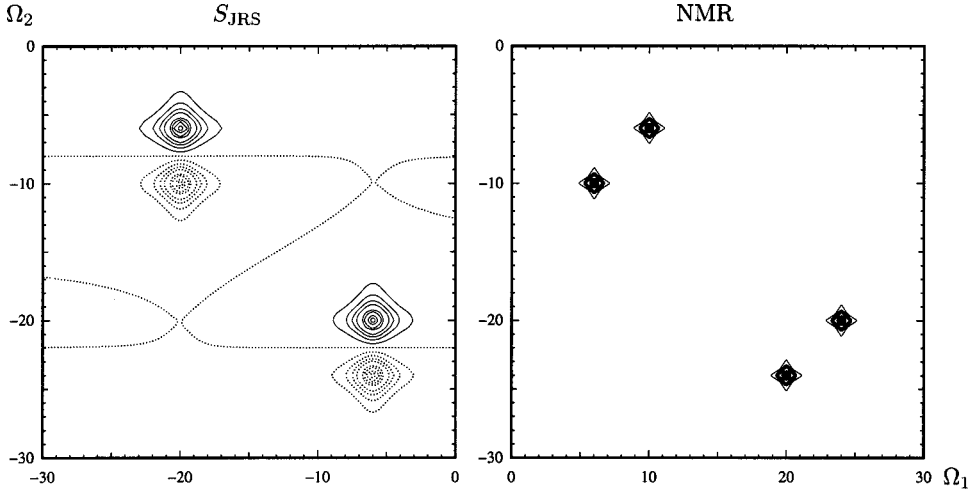

FIG. 6. Combinations of two-dimensional spectra observed in different directions yield for $S_{\rm JRS}=S_{\rm I}(-\Omega_1,\Omega_2)-S_{\rm II}(\Omega_1,\Omega_2)+S_{\rm III}(\Omega_1,\Omega_2)$ (left) a technique with the same information content as NMR *J*-resolved spectroscopy [right, compare Fig. 1(c)]. Solid contour lines represent a positive signal while negative contours are dotted.

It is crucial to detect the full (heterodyne) signal and not merely its absolute value to be able to construct linear combinations of signals in different directions in which certain selected peaks cancel.

F. Double quantum spectroscopy

All the pulse sequences discussed so far used the second and third pulse as the mixing block. The second possibility to obtain a two-dimensional spectrum from a three-pulse sequence is to consider the first two pulses as the preparation sequence and to obtain the two frequency domains from τ_2 and τ_3. In this case the two responses $S_{\mathrm{I,II}}$ only yield zero frequency peaks in the first frequency domain since the system is in a 0QC state during τ_2. These signals are usually unwanted since they are essentially one-dimensional and therefore suppressed in 2D NMR. However, directional detection allows to directly observe signal S_{III} which corresponds to the simplest multiple quantum technique in NMR, double quantum spectroscopy. We can therefore identify

$$S_{\mathrm{DQS}}(\tau_2,\tau_3)=S_{\mathrm{III}}(\tau_p,\tau_2,\tau_3), \tag{64}$$

where the two time domains are given by τ_2 and τ_3 while $\tau_1=\tau_p$ is a constant delay. In this technique the duration of the delay τ_p can be adjusted with respect to the coupling J to maximize the transfer to the 2QC during the preparation block. The system then evolves with the sum frequency of $\omega_\alpha+\omega_\beta$ during τ_2 giving rise to a spectrum that contains peaks at about twice the frequency in the first domain as a usual single quantum experiment. The mixing pulse (pulse three) then correlates the 2QC with the connected 1QCs.

V. CONCLUSIONS

We have developed a description of optical pulse experiments using well-separated, time-ordered pulses in the weak field limit for coupled two-level systems that is closely related to the NMR product operator formalism. Describing the action of weak pulses in terms of transformations in the basis of Pauli matrices or creation and annihilation operators is based on the RWA for resonant spectroscopy and the relationship $\Delta\omega\ll\omega_1\ll\omega_0$, where $\Delta\omega$ is the width of the spectrum, ω_1 the Rabi frequency, and ω_0 the central transition frequency. The transformation rules for product states of basis operators offer a very compact description of the interaction of the system with the electromagnetic field of the pulses without dealing with the detailed features of the pulses.

Models for the interaction between optical two-level systems in molecular crystals and aggregates usually are based on the resonant J-coupling Hamiltonian

$$\mathsf{H}_{J,\mathrm{res}}=J_{\alpha\beta}(\mathsf{B}_\alpha^\dagger\mathsf{B}_\beta+\mathsf{B}_\alpha\mathsf{B}_\beta^\dagger). \tag{65}$$

Here the I_z terms in the full isotropic coupling Hamiltonian (13) are neglected. Simple models of this kind are based on transition dipole coupling mechanisms (see e.g., Refs. 33, 34). This Hamiltonian leads to the formation of exciton states and techniques for its treatment are well-developed.[13,15] The present model [Eq. (13)] is different and also includes diagonal couplings. For nonresonant couplings, which is the limit opposite to Eq. (65), the perturbative expansion in J (weak J-coupling limit) and the use of product states of localized basis states for the chromophores allows a real-space interpretation of the action of the pulse sequence. This considerably simplifies the design of specialized pulse sequences for the extraction of specific system parameters like transition frequencies and J-couplings and yields a more intuitive picture than possible using the global eigenstates. While the description of weak pulse sequences developed in Sec. III is valid for arbitrary coupling Hamiltonians, it becomes most powerful when combined with the weak J-coupling Hamiltonian of Sec. II. The formalism then directly yields analytical expressions for the evolution of the density matrix and for the polarization. Sequences designed in the weak J limit may retain their essential features for strong J as well. In two-color experiments nonresonant couplings provide the dominant coupling mechanism that can be exploited for coherence transfer.

The selection of coherence transfer pathways which is obtained in NMR by phase-cycling is possible in optical spectroscopy through directional detection. Signals detected in different directions can be linearly combined to simplify the resulting 2D spectra, yielding techniques that resemble NMR results from pulse sequences involving strong π-pulses. The combination of directional detection, linear combination of signals from different spatial directions, and cycling of pulse phases gives a high degree of control over the selection of coherence transfer pathways. To gain this control it is necessary to measure the full complex signal by heterodyne detection and not only the absolute value spectrum. This is common practice in NMR. A further advantage of heterodyne detection is that after appropriate phase correction and data processing, it can also yield pure absorptive spectra which have considerably higher resolution than absolute value spectra.

We have identified close optical analogs of the most important liquid state NMR three pulse techniques (COSY, NOESY, DQS). Future research will involve the development of new pulse sequences that carefully account for the differences between NMR and optical spectroscopy. Two-color experiments analogous to heteronuclear NMR spectroscopy are one interesting possibility and pulse experiments that are tailored to certain classes of compounds (proteins, polymers) could be developed.[2] The systematic extension of the current formalism to arbitrary multi-level systems should not pose fundamental difficulties and will enable the treatment of a larger variety of systems, including vibrational systems with moderate anharmonicities. A further topic that should be studied is the description of pulse sequence blocks in terms of average Hamiltonians that yield effective transformations for the whole pulse train. This approach has been used effectively in solid state NMR[1,35] and can become important in dealing with the arbitrarily oriented dipoles in optical spectroscopy. Techniques that effectively deal with small pulse flip angles, offset effects, and echo detection have been developed in multidimensional EPR spectroscopy[36,37] and might stimulate further development of optical pulse techniques.

ACKNOWLEDGMENTS

The support of the National Institutes of Health (GM59230-01A2) and the National Science foundation (CHE-9814061) is gratefully acknowledged. One of the authors (C.S.) thanks the Alexander von Humboldt Foundation for a Feodor Lynen fellowship.

APPENDIX A: PAULI MATRICES, SPIN-OPERATORS, CREATION AND ANNIHILATION OPERATORS

In this appendix we survey some well-known operator properties and relations that are widely used in NMR and that are needed for the operator transformation rules in Sec. III. For the description of two-level systems we use operator bases that contain Cartesian $(\mathsf{I}_x,\mathsf{I}_y,\mathsf{I}_z)$ or creation and annihilation $(\mathsf{B}^\dagger,\mathsf{B})$ operators depending on which basis yields the more compact description. The two states forming the Hilbert space on which the operators are defined are typically called $\{|\alpha\rangle,|\beta\rangle\}$ in NMR and $\{|-\rangle,|+\rangle\}$ in optical spectroscopy. As a common notation we will use $\{|a\rangle,|b\rangle\}$ in the following. Any Hermitian operator on this Hilbert space can be expanded in terms of the identity operator I and the Pauli matrices σ_x, σ_y, and σ_z. In NMR the spin operators are usually referred to as I_x, I_y, and I_z, which are the Pauli matrices with appropriate normalization, satisfying the well-known commutation relations (we use units in which $\hbar=1$):

$$[\mathsf{I}_x,\mathsf{I}_y]=i\,\mathsf{I}_z \quad \text{and cyclic permutations of } (x,y,z). \tag{A1}$$

The creation and annihilation operators, also called shift or flip operators, are given by

$$\mathsf{I}^+=\mathsf{I}_x+i\mathsf{I}_y \quad \text{and} \quad \mathsf{I}^-=\mathsf{I}_x-i\,\mathsf{I}_y. \tag{A2}$$

They fulfill the following commutator relationships,

$$\begin{aligned}&[\mathsf{I}^\pm,\mathsf{I}_x]=\pm\mathsf{I}_z, \quad [\mathsf{I}^\pm,\mathsf{I}_y]=i\,\mathsf{I}_z,\\ &[\mathsf{I}^\pm,\mathsf{I}_z]=\mp\mathsf{I}^\pm, \quad [\mathsf{I}^+,\mathsf{I}^-]=2\,\mathsf{I}_z.\end{aligned} \tag{A3}$$

To make the comparison with the optical spectroscopy notation easier we denote $\mathsf{B}^\dagger=\mathsf{I}^+$ and $\mathsf{B}=\mathsf{I}^-$. The inverse relations are given by

$$\mathsf{I}_x=\frac{1}{2}(\mathsf{B}^\dagger+\mathsf{B}) \quad \text{and} \quad \mathsf{I}_y=-\frac{i}{2}(\mathsf{B}^\dagger-\mathsf{B}). \tag{A4}$$

The spin operators fulfill further relations:

$$\mathsf{I}_x^2=\mathsf{I}_y^2=\mathsf{I}_z^2=\tfrac{1}{4}\mathsf{I}, \tag{A5}$$

$$(\mathsf{B}^\dagger)^2=\mathsf{B}^2=0, \tag{A6}$$

$$\mathsf{I}_x\mathsf{I}_y=\frac{i}{2}\mathsf{I}_z \quad \text{and cyclic permutations of } (x,y,z), \tag{A7}$$

$$\mathsf{I}_y\mathsf{I}_x=-\frac{i}{2}\mathsf{I}_z \quad \text{and cyclic permutations of } (x,y,z). \tag{A8}$$

From this follows $([A,B]_+=AB+BA)$

$$\mathsf{I}_z=\tfrac{1}{2}[\mathsf{B}^\dagger,\mathsf{B}], \tag{A9}$$

$$\mathsf{I}=[\mathsf{B}^\dagger,\mathsf{B}]_+. \tag{A10}$$

The transformation properties under z-rotations are given by[1,23]

$$\mathsf{R}_z(\varphi)=\exp(i\,\mathsf{I}_z\varphi)=\mathsf{R}_z^{-1}(-\varphi), \tag{A11}$$

$$\mathsf{I}_x'=\mathsf{R}_z^{-1}(\varphi)\mathsf{I}_x\mathsf{R}_z(\varphi)=\mathsf{I}_x\cos\varphi+\mathsf{I}_y\sin\varphi, \tag{A12}$$

$$\mathsf{I}_y'=\mathsf{R}_z^{-1}(\varphi)\mathsf{I}_y\mathsf{R}_z(\varphi)=-\mathsf{I}_x\sin\varphi+\mathsf{I}_y\cos\varphi, \tag{A13}$$

$$\mathsf{I}_z'=\mathsf{R}_z^{-1}(\varphi)\mathsf{I}_z\mathsf{R}_z(\varphi)=\mathsf{I}_z, \tag{A14}$$

$$(\mathsf{B}^\dagger)'=\mathsf{R}_z^{-1}(\varphi)\mathsf{B}^\dagger\mathsf{R}_z(\varphi)=\mathsf{B}^\dagger e^{-i\varphi} \tag{A15}$$

$$\mathsf{B}'=\mathsf{R}_z^{-1}(\varphi)\mathsf{B}\mathsf{R}_z(\varphi)=\mathsf{B}e^{i\varphi}. \tag{A16}$$

APPENDIX B: HAMILTONIAN FOR A DRIVEN SPIN-$\frac{1}{2}$ AND A TWO LEVEL SYSTEM

In this Appendix we present the derivation of the effective rotating-frame Hamiltonian of a spin-$\frac{1}{2}$ in an electromagnetic field, following the treatment in Ref. 23. The resulting Hamiltonian has the same structure as the optical two-level Hamiltonian of Sec. II.

The magnetic moment operator of a spin-$\frac{1}{2}$ system is given by Eq. (4).[23,24] It is isotropic and has the same magnitude for all spins of the same isotope. The Hamiltonian for a spin in a magnetic field $\boldsymbol{\mathcal{H}}$ is

$$\mathsf{H}=-\boldsymbol{\mu}\cdot\boldsymbol{\mathcal{H}}(t). \tag{B1}$$

We assume that the spin is placed in a strong static magnetic field $\boldsymbol{\mathcal{H}}_0=\mathcal{H}_0\,\mathbf{e}_z$ parallel to the z-axis which becomes the quantizationa axis. All spins are then aligned either parallel or anti-parallel with respect to the z-axis which gives rise to the Zeeman splitting between the states $|\alpha\rangle$ and $|\beta\rangle$. The corresponding energy difference is the Larmor frequency $\omega_0=\gamma\mathcal{H}_0$. A circularly polarized rf-pulse with rotating magnetic field $\boldsymbol{\mathcal{H}}_1(t)$ is applied in the x-y plane with frequency ω and phase φ (here, effectively $\mathbf{k}=0$),

$$\boldsymbol{\mathcal{H}}_1(t)=\mathcal{H}_1(t)[\mathbf{e}_x\cos(\omega t+\varphi)+\mathbf{e}_y\sin(\omega t+\varphi)]. \tag{B2}$$

Adding both fields $\boldsymbol{\mathcal{H}}(t)=\boldsymbol{\mathcal{H}}_0+\boldsymbol{\mathcal{H}}_1(t)$ the Hamiltonian reads

$$\mathsf{H}=-\omega_0\mathsf{I}_z-\gamma\mathcal{H}_1(t)\underbrace{[\mathsf{I}_x\cos(\omega t+\varphi)+\mathsf{I}_y\sin(\omega t+\varphi)]}_{\mathsf{P}(\omega t+\varphi)}. \tag{B3}$$

The operator $\mathsf{P}(\omega t+\varphi)$ describing the action of the pulse on the spin-$\frac{1}{2}$ system has a simple interpretation in terms of infinitesimal rotations as can be seen by comparing $\mathsf{P}(\omega t+\varphi)$ with Eqs. (A12) and (A13)

$$\mathsf{P}(\omega t+\varphi)=\begin{cases}\mathsf{R}\mathsf{I}_x\mathsf{R}^{-1} & \text{for} \quad \varphi=0\\ \mathsf{R}\mathsf{I}_y\mathsf{R}^{-1} & \text{for} \quad \varphi=\dfrac{\pi}{2}\\ \mathsf{R}(-\mathsf{I}_x)\mathsf{R}^{-1} & \text{for} \quad \varphi=\pi\\ \mathsf{R}(-\mathsf{I}_y)\mathsf{R}^{-1} & \text{for} \quad \varphi=3\dfrac{\pi}{2}\end{cases} \tag{B4}$$

$$\text{with:} \quad \mathsf{R}=\mathsf{R}_z(-\omega t). \tag{B5}$$

The Rabi frequency is given by $\omega_1=\gamma\mathcal{H}_1(t)$. Integrating over the pulse yields the flip angle $\theta=\gamma\int\mathcal{H}_1(t)\,dt$.

In the following we will assume for simplicity a rectangular pulse during which $\mathcal{H}_1(t)=\mathcal{H}_1$ is constant and zero before and after the pulse. The Liouville–von Neuman equation $\dot{\rho}=[\mathsf{H},\rho]$ describing the dynamics of the spin system during the pulse is then given by

$$\dot{\rho}=-i(\omega_0[\mathsf{I}_z,\rho]+\omega_1[\mathsf{R}\mathsf{I}_k\mathsf{R}^{-1},\rho]), \tag{B6}$$

where the index k can be either x, y, $-x$, or $-y$. The equation of motion can be simplified by the rotating frame transformation $\rho\rightarrow\mathsf{R}\rho\mathsf{R}^{-1}$:[23]

$$-i\omega[\mathsf{I}_z,\mathsf{R}\rho\mathsf{R}^{-1}]+\mathsf{R}\dot{\rho}\mathsf{R}^{-1}$$
$$=-i(\omega_0[\mathsf{I}_z,\mathsf{R}\rho\mathsf{R}^{-1}]+\omega_1[\mathsf{R}\mathsf{I}_k\mathsf{R}^{-1},\mathsf{R}\rho\mathsf{R}^{-1}]). \tag{B7}$$

Multiplication of Eq. (B7) from the left by R^{-1} and from the right by R and using the fact that $[\mathsf{R},\mathsf{I}_z]=0$ yields the equation of motion in the rotating frame,

$$-i\omega[\mathsf{I}_z,\rho]+\dot{\rho}=-i(\omega_0[\mathsf{I}_z,\rho]+\omega_1[\mathsf{I}_k,\rho]). \tag{B8}$$

This result can be simplified by introducing the effective Hamiltonian $\mathsf{H}_{\mathrm{eff}}$,

$$\dot{\rho}=-i[\mathsf{H}_{\mathrm{eff}},\rho] \quad \text{where} \quad \mathsf{H}_{\mathrm{eff}}=(\omega_0-\omega)\mathsf{I}_z+\omega_1\mathsf{I}_k. \tag{B9}$$

In terms of creation and annihilation operators the effective Hamiltonian can be written as

$$\mathsf{H}_{\mathrm{eff}}^{\alpha}=\frac{1}{2}(\omega_\alpha-\omega)[\mathsf{B}_\alpha^\dagger,\mathsf{B}_\alpha]+\frac{\omega_1}{2}(\cos\varphi(\mathsf{B}_\alpha^\dagger+\mathsf{B}_\alpha)$$
$$-i\sin\varphi(\mathsf{B}_\alpha^\dagger-\mathsf{B}_\alpha)). \tag{B10}$$

Rearranging Eq. (B10) results in Eq. (8).

APPENDIX C: OPTICAL RESPONSE TO A THREE-PULSE SEQUENCE

We consider the weak J-coupling Hamiltonian Eq. (17) for coupled two-level systems. The initial (low temperature) density matrix is

$$\rho_0\propto\prod_\alpha(\mathsf{I}^\alpha-\mathsf{I}_z^\alpha), \tag{C1}$$

while the high temperature approximation in NMR would yield an initial density matrix $\rho_0\propto\Sigma_\alpha\mathsf{I}_z^\alpha$. The evolution under the three-pulse sequence was computed by

$$\rho_0\xrightarrow{\phi_1^\omega}\xrightarrow{\mathsf{H}_Z\tau_1}\xrightarrow{\mathsf{H}_J\tau_1}\rho_{\tau_1}$$
$$\xrightarrow{\phi_2^\omega}\xrightarrow{\mathsf{H}_Z\tau_2}\xrightarrow{\mathsf{H}_J\tau_2}\rho_{\tau_1+\tau_2}$$
$$\xrightarrow{\phi_3^\omega}\xrightarrow{\mathsf{H}_Z\tau_3}\xrightarrow{\mathsf{H}_J\tau_3}\rho_{\tau_1+\tau_2+\tau_3} \tag{C2}$$

and an overall relaxation term with rate Γ was added [compare Eq. (55)]. The polarization Eq. (53) is obtained as

$$P^{(3)}(\tau_1,\tau_2,\tau_3)=\mathrm{tr}\left\{\rho_{\tau_1+\tau_2+\tau_3}\sum_\alpha\boldsymbol{\mu}_\alpha^{ab}\mathsf{B}_\alpha+\boldsymbol{\mu}_\alpha^{ba}\mathsf{B}_\alpha^\dagger\right\}. \tag{C3}$$

Detection with an additional heterodyne pulse with envelope $\boldsymbol{\mathcal{E}}_h(t)$ and phase ϕ_h yields a signal which can be split into three terms that comprise contributions with common phase factors and their conjugate complex counterparts resulting from the $\mathsf{B}^\dagger$ and B contributions to the dipole operator, respectively

$$S(\tau_1,\tau_2,\tau_3)=\sum_{k=\mathrm{I,II,III}}S_k(\tau_1,\tau_2,\tau_3)+S_k'(\tau_1,\tau_2,\tau_3). \tag{C4}$$

The three components $S_{\mathrm{I,II,III}}$ are observable in the different phase matched directions $\mathbf{k}_{\mathrm{I}}=-\mathbf{k}_1+\mathbf{k}_2+\mathbf{k}_3$, $\mathbf{k}_{\mathrm{II}}=\mathbf{k}_1-\mathbf{k}_2+\mathbf{k}_3$, and $\mathbf{k}_{\mathrm{III}}=\mathbf{k}_1+\mathbf{k}_2-\mathbf{k}_3$ and can also be obtained from the sum-over-states expressions.[13] Using the abbreviations

$$\omega_\alpha^-=\omega_\alpha-\frac{1}{2}\sum_{\gamma\neq\alpha}J_{\alpha\gamma}, \tag{C5}$$

$$\omega_\alpha^\beta=\omega_\alpha+\frac{1}{2}\left(J_{\alpha\beta}-\sum_{\gamma\neq\alpha,\beta}J_{\alpha\gamma}\right), \tag{C6}$$

$$2\,\Omega_{\alpha\beta}=\omega_\alpha+\omega_\beta-\sum_{\gamma\neq\alpha,\beta}J_{\alpha\gamma}, \tag{C7}$$

$$2\,\Delta_{\alpha\beta}=\omega_\alpha-\omega_\beta+\frac{1}{2}\sum_{\gamma\neq\alpha,\beta}(J_{\beta\gamma}-J_{\alpha\gamma}), \tag{C8}$$

and $\mathsf{V}_{h,\alpha}=\boldsymbol{\mu}_\alpha^{ab}\cdot\boldsymbol{\mathcal{E}}_h$ the signals are given by:

$$S_{\mathrm{I}}(\tau_1,\tau_2,\tau_3)=-ie^{i(\phi_h-\phi_1+\phi_2+\phi_3)}e^{-\Gamma(\tau_1+\tau_2+\tau_3)}\sum_{\alpha\neq\beta}[2\,\mathsf{V}_{h,\alpha}^-\mathsf{V}_{3,\alpha}^+\mathsf{V}_{2,\alpha}^+\mathsf{V}_{1,\alpha}^-\exp(-i(\omega_\alpha^-(\tau_3-\tau_1)))$$
$$+2\,\mathsf{V}_{h,\beta}^-\mathsf{V}_{3,\beta}^+\mathsf{V}_{2,\beta}^+\mathsf{V}_{1,\beta}^-\exp(-i(\omega_\beta^-(\tau_3-\tau_1)))+\mathsf{V}_{h,\alpha}^-\mathsf{V}_{3,\beta}^+\mathsf{V}_{2,\alpha}^+\mathsf{V}_{1,\beta}^-\exp(-i(-\omega_\beta^-\tau_1+2\,\Delta_{\alpha\beta}\tau_2+\omega_\alpha^-\tau_3))$$
$$-\mathsf{V}_{h,\alpha}^-\mathsf{V}_{3,\beta}^+\mathsf{V}_{2,\alpha}^+\mathsf{V}_{1,\beta}^-\exp(-i(-\omega_\beta^-\tau_1+2\,\Delta_{\alpha\beta}\tau_2+\omega_\alpha^\beta\tau_3))+\mathsf{V}_{h,\beta}^-\mathsf{V}_{3,\alpha}^+\mathsf{V}_{2,\beta}^+\mathsf{V}_{1,\alpha}^-$$
$$\times\exp(-i(-\omega_\alpha^-\tau_1-2\,\Delta_{\alpha\beta}\tau_2+\omega_\beta^-\tau_3))-\mathsf{V}_{h,\beta}^-\mathsf{V}_{3,\alpha}^+\mathsf{V}_{2,\beta}^+\mathsf{V}_{1,\alpha}^-\exp(-i(-\omega_\alpha^-\tau_1-2\,\Delta_{\alpha\beta}\tau_2+\omega_\beta^\alpha\tau_3))$$
$$+\mathsf{V}_{h,\alpha}^-\mathsf{V}_{3,\alpha}^+\mathsf{V}_{2,\beta}^+\mathsf{V}_{1,\beta}^-\exp(-i(-\omega_\beta^-\tau_1+\omega_\alpha^-\tau_3))-\mathsf{V}_{h,\alpha}^-\mathsf{V}_{3,\alpha}^+\mathsf{V}_{2,\beta}^+\mathsf{V}_{1,\beta}^-\exp(-i(-\omega_\beta^-\tau_1+\omega_\alpha^\beta\tau_3))$$
$$+\mathsf{V}_{h,\beta}^-\mathsf{V}_{3,\beta}^+\mathsf{V}_{2,\alpha}^+\mathsf{V}_{1,\alpha}^-\exp(-i(-\omega_\alpha^-\tau_1+\omega_\beta^-\tau_3))-\mathsf{V}_{h,\beta}^-\mathsf{V}_{3,\beta}^+\mathsf{V}_{2,\alpha}^+\mathsf{V}_{1,\alpha}^-\exp(-i(-\omega_\alpha^-\tau_1+\omega_\beta^\alpha\tau_3))], \tag{C9}$$

$$S_{\mathrm{II}}(\tau_1,\tau_2,\tau_3) = -ie^{i(\phi_h+\phi_1-\phi_2+\phi_3)}e^{-\Gamma(\tau_1+\tau_2+\tau_3)}\sum_{\alpha\neq\beta}[2\,V^-_{h,\alpha}V^+_{3,\alpha}V^-_{2,\alpha}V^+_{1,\alpha}\exp(-i(\omega^-_\alpha(\tau_3+\tau_1)))$$
$$+2\,V^-_{h,\beta}V^+_{3,\beta}V^-_{2,\beta}V^+_{1,\beta}\exp(-i(\omega^-_\beta(\tau_3+\tau_1)))+V^-_{h,\alpha}V^+_{3,\beta}V^-_{2,\beta}V^+_{1,\alpha}\exp(-i(\omega^-_\alpha\tau_1+2\,\Delta_{\alpha\beta}\tau_2+\omega^-_\alpha\tau_3))$$
$$-V^-_{h,\alpha}V^+_{3,\beta}V^-_{2,\beta}V^+_{1,\alpha}\exp(-i(\omega^-_\alpha\tau_1+2\,\Delta_{\alpha\beta}\tau_2+\omega^\beta_\alpha\tau_3))+V^-_{h,\beta}V^+_{3,\alpha}V^-_{2,\alpha}V^+_{1,\beta}$$
$$\times\exp(-i(\omega^-_\beta\tau_1-2\,\Delta_{\alpha\beta}\tau_2+\omega^-_\beta\tau_3))-V^-_{h,\beta}V^+_{3,\alpha}V^-_{2,\alpha}V^+_{1,\beta}\exp(-i(\omega^-_\beta\tau_1-2\,\Delta_{\alpha\beta}\tau_2+\omega^\alpha_\beta\tau_3))$$
$$+V^-_{h,\alpha}V^+_{3,\alpha}V^-_{2,\beta}V^+_{1,\beta}\exp(-i(\omega^-_\beta\tau_1+\omega^-_\alpha\tau_3))-V^-_{h,\alpha}V^+_{3,\alpha}V^-_{2,\beta}V^+_{1,\beta}\exp(-i(\omega^-_\beta\tau_1+\omega^\beta_\alpha\tau_3))$$
$$+V^-_{h,\beta}V^+_{3,\beta}V^-_{2,\alpha}V^+_{1,\alpha}\exp(-i(\omega^-_\alpha\tau_1+\omega^-_\beta\tau_3))-V^-_{h,\beta}V^+_{3,\beta}V^-_{2,\alpha}V^+_{1,\alpha}\exp(-i(\omega^-_\alpha\tau_1+\omega^\alpha_\beta\tau_3))], \tag{C10}$$

$$S_{\mathrm{III}}(\tau_1,\tau_2,\tau_3) = -ie^{i(\phi_h+\phi_1+\phi_2-\phi_3)}e^{-\Gamma(\tau_1+\tau_2+\tau_3)}\sum_{\alpha\neq\beta}[V^-_{h,\alpha}V^-_{3,\beta}V^+_{2,\beta}V^+_{1,\alpha}\exp(-i(\omega^-_\alpha\tau_1+2\,\Omega_{\alpha\beta}\tau_2+\omega^-_\alpha\tau_3))$$
$$-V^-_{h,\alpha}V^-_{3,\beta}V^+_{2,\beta}V^+_{1,\alpha}\exp(-i(\omega^-_\alpha\tau_1+2\,\Omega_{\alpha\beta}\tau_2+\omega^\beta_\alpha\tau_3))+V^-_{h,\beta}V^-_{3,\alpha}V^+_{2,\beta}V^+_{1,\alpha}\exp(-i(\omega^-_\alpha\tau_1+2\,\Omega_{\alpha\beta}\tau_2$$
$$+\omega^-_\beta\tau_3))-V^-_{h,\beta}V^-_{3,\alpha}V^+_{2,\beta}V^+_{1,\alpha}\exp(-i(\omega^-_\alpha\tau_1+2\,\Omega_{\alpha\beta}\tau_2+\omega^\alpha_\beta\tau_3))+V^-_{h,\alpha}V^-_{3,\beta}V^+_{2,\alpha}V^+_{1,\beta}\exp(-i(\omega^-_\beta\tau_1$$
$$+2\,\Omega_{\alpha\beta}\tau_2+\omega^-_\alpha\tau_3))-V^-_{h,\alpha}V^-_{3,\beta}V^+_{2,\alpha}V^+_{1,\beta}\exp(-i(\omega^-_\beta\tau_1+2\,\Omega_{\alpha\beta}\tau_2+\omega^\beta_\alpha\tau_3))+V^-_{h,\beta}V^-_{3,\alpha}V^+_{2,\alpha}V^+_{1,\beta}$$
$$\times\exp(-i(\omega^-_\beta\tau_1+2\,\Omega_{\alpha\beta}\tau_2+\omega^-_\beta\tau_3))-V^-_{h,\beta}V^-_{3,\alpha}V^+_{2,\alpha}V^+_{1,\beta}\exp(-i(\omega^-_\beta\tau_1+2\,\Omega_{\alpha\beta}\tau_2+\omega^\alpha_\beta\tau_3))]. \tag{C11}$$

For a system of two coupled two-level systems the above relationships reduce to the ones given in the level scheme in Fig. 2 with the corresponding 2D signals given in Fig. 4.

It can be easily seen that for $\tau_1=0$ the signals S_{I} and S_{II} become identical (up to interchanging the pulse indices 1 and 2) and for $\tau_2=0$ signals S_{II} and S_{III} carry the same information. The resulting four techniques are closely related to photon echo, reverse photon echo, transient grating, reverse transient grating that have been identified earlier.[15,16] The techniques discussed here differ from the these techniques in that in the current case time-ordering is preserved. The refocusing echo observed in the standard PE technique ($\tau_2=0$) can be most easily seen in the two first terms of S_{II} which depend on $\tau_3-\tau_1$, yielding an exact recurrence at $\tau_3=\tau_1$ for any inhomogeneous distribution of ω_α and ω_β.

[1] R. R. Ernst, G. Bodenhausen, and A. Wokaun, *Principles of Nuclear Magnetic Resonance in One and Two Dimensions* (Clarendon, Oxford, 1987).
[2] J. Cavanagh, W. J. Fairbrother, I. Palmer, G. Arthur, and N. J. Skelton, *Protein NMR Spectroscopy: Principles and Practice* (Academic, San Diego, 1996).
[3] *Ultrafast Phenomena XII*, edited by T. Elsaesser, S. Mukamel, M. M. Murnane, and N. F. Scherer (Springer, Berlin, 2001).
[4] J. D. Hybl, Y. Christophe, and D. M. Jonas, Chem. Phys., **266**, 295, (2001).
[5] M. C. Asplund, M. T. Zanni, and R. M. Hochstrasser, Proc. Natl. Acad. Sci. U.S.A. **97**, 8219 (2000).
[6] K. A. Merchant, D. E. Thompson, and M. D. Fayer, J. Chem. Phys. **115**, 317 (2001); Phys. Rev. Lett. **86**, 3899 (2001).
[7] P. Hamm, M. Lim, W. DeGrado, and R. Hochstrasser, J. Chem. Phys. **112**, 1907 (2000).
[8] K. Okumura, A. Tokmakoff, and Y. Tanimura, J. Chem. Phys. **111**, 492 (1999).
[9] K. D. Rector, A. S. Kwok, C. Ferrante, A. Tokmakoff, C. W. Rella, and M. D. Fayer, J. Chem. Phys. **106**, 10027 (1997).
[10] T. H. Joo, Y. W. Jia, J. Y. Yu, D. M. Jonas, and G. R. Fleming, J. Phys. Chem. **100**, 2399 (1996).
[11] E. Brown, I. Pastirk, B. Grimberg, V. Lozovoy, and M. Dantus, J. Chem. Phys. **111**, 3779 (1999).
[12] R. Zadoyan and V. A. Apkarian, Chem. Phys. Lett. **326**, 1 (2000).
[13] S. Mukamel, *Principles of Nonlinear Optical Spectroscopy* (Oxford University Press, New York, 1995).
[14] Y. Tanimura and S. Mukamel, J. Chem. Phys. **99**, 9496 (1993).
[15] V. Chernyak, W. M. Zhang, and S. Mukamel, J. Chem. Phys. **109**, 9587 (1998).
[16] W. M. Zhang, V. Chernyak, and S. Mukamel, J. Chem. Phys. **110**, 5011 (1999).
[17] S. Mukamel, Annu. Rev. Phys. Chem. **51**, 691 (2000).
[18] R. R. Ernst, Angew. Chem. Int. Ed. Engl. **31**, 805 (1992).
[19] O. W. Sørensen, Prog. Nucl. Magn. Reson. Spectrosc. **21**, 503 (1989).
[20] D. Keusters, H.-S. Tan, and W. Warren, J. Phys. Chem. A **103**, 10369 (1999).
[21] W. Warren and A. Zewail, J. Chem. Phys. **75**, 5956 (1981); **78**, 2279 (1983); **78**, 2298 (1983).
[22] R. P. Feynman, J. F. L. Vernon, and R. W. Hellwarth, J. Appl. Phys. **28**, 49 (1957).
[23] C. P. Slichter, *Principles of Magnetic Resonance* (Springer, Berlin, 1990).
[24] A. Abragam, *The Principles of Nuclear Magnetism* (Clarendon, Oxford, 1961).
[25] L. Allen and J. H. Eberly, *Optical Resonance and Two-Level Atoms* (Wiley, New York, 1975).
[26] B. W. Shore, *The Theory of Coherent Atomic Excitation* (Wiley, New York, 1990).
[27] S. Mukamel, Phys. Rev. A **61**, 021804/1 (2000).
[28] A. Albrecht, J. Hybl, S. Gallagher Faeder, and D. Jones, J. Chem. Phys. **111**, 10934 (1999).
[29] S. Mukamel, A. Piryatinski, and V. Chernyak, Acc. Chem. Res. **32**, 145 (1999).
[30] B. I. Grimberg, V. V. Lozovoy, M. Dantus, and S. Mukamel, J. Phys. Chem. (2001), submitted.
[31] S. J. Glaser, T. Schulte-Herbrüggen, M. Sieveking, O. Schedletzky, N. C. Nielsen, O. W. Sørensen, and C. Griesinger, Science **280**, 421 (1998).
[32] S. Mukamel, A. Piryatinski, and V. Chernyak, J. Chem. Phys. **110**, 1711 (1999).
[33] S. Krimm and Y. Abe, Proc. Natl. Acad. Sci. U.S.A. **69**, 2788 (1972).
[34] A. S. Davydov, *Theory of Molecular Excitons* (Plenum, New York, 1971).
[35] M. Mehring, *Principles of High Resolution NMR in Solids* (Springer, Berlin, 1983).
[36] J. H. Freed, Annu. Rev. Phys. Chem. **51**, 655 (2000).
[37] S. Van Doorslaer and A. Schweiger, Naturwissenschaften **87**, 245 (2000).